HHS Public Access

Author manuscript

Curr Med Chem. Author manuscript; available in PMC 2023 April 07.

Published in final edited form as:

Curr Med Chem. 2022 August 06; 29(28): 4862–4890. doi:10.2174/0929867329666220329204054.

Essential Principles and Recent Progress in the Development of TSPO PET Ligands for Neuroinflammation Imaging

Monica Viviano[1], **Elisabetta Barresi**[2], **Fabrice G. Siméon**[3], **Barbara Costa**[2], **Sabrina Taliani**[2], **Federico Da Settimo**[2], **Victor W. Pike**[3], **Sabrina Castellano**[1,*]

[1]Department of Pharmacy, University of Salerno, 84084 Fisciano (SA), Italy

[2]Department of Pharmacy, University of Pisa, 56126, Pisa, Italy

[3]Molecular Imaging Branch, National Institute of Mental Health, National Institutes of Health, Bethesda, MD 20892, USA

Abstract

The translocator protein 18kDa (TSPO) is expressed in the outer mitochondrial membrane and is implicated in several functions, including cholesterol transport and steroidogenesis. Under normal physiological conditions, TSPO is present in very low concentrations in the human brain but is markedly upregulated in response to brain injury and inflammation. This upregulation is strongly associated with activated microglia. Therefore, TSPO is particularly suited for assessing active gliosis associated with brain lesions following injury or disease. For over three decades, TSPO has been studied as a biomarker. Numerous radioligands for positron emission tomography (PET) that target TSPO have been developed for imaging inflammatory progression in the brain. Although [^{11}C]PK11195, the prototypical first-generation PET radioligand, is still widely used for *in vivo* studies, mainly now as its single more potent *R*-enantiomer, it has severe limitations, including low sensitivity and poor amenability to quantification. Second-generation radioligands are characterized by higher TSPO specific signals but suffer from other drawbacks, such as sensitivity to the TSPO single nucleotide polymorphism (SNP) rs6971. Therefore, their applications in human studies have the burden of needing to genotype subjects. Consequently, recent efforts are focused on developing improved radioligands that combine the optimal features of the second generation with the ability to overcome the differences in binding affinities across the population. This review presents essential principles in the design and development of TSPO PET ligands and discusses prominent examples among the main chemotypes.

Keywords

TSPO; neuroinflammation; imaging; PET; radioligand; drug development; diagnostic marker

*Address correspondence to this author at the Department of Pharmacy, University of Salerno, 84084 Fisciano (SA), Italy; Tel: +39 089 969244; scastellano@unisa.it.

AUTHORS' CONTRIBUTION

All authors listed have contributed substantially to the manuscript. SC, FDS and VWP in writing the manuscript, MV, EB and FGS in data collection, BC and ST in data analysis and interpretation

CONFLICT OF INTEREST

The authors declares no conflict of interest, financial or otherwise.

1. INTRODUCTION

The translocator protein 18kDa (TSPO), formerly known as the peripheral-type benzodiazepine receptor (PBR), is mainly located at the outer mitochondrial membrane [1]. TSPO is an evolutionary well--conserved and tryptophan-rich 169-amino acid protein and consists of five transmembrane α-helices, each composed of 21 residues that span the entire membrane bilayer with a carboxyl terminus located outside the mitochondria and an amino-terminal inside. Li *et al.* first described a cholesterol recognition amino acid consensus sequence (CRAC) in the carboxyl terminus of TSPO [2]. TSPO generally functions as a monomer [3], but forms oligomers with itself (homo-oligomers) or other proteins, such as the voltage-dependent anion channel (VDAC), adenine nucleotide translocase (ANT), and steroidogenic acute regulatory protein (StAR), thus forming what has become known as the mitochondrial permeability transition pore (MPTP) [4].

In recent years, structural information on TSPO has been obtained by different methods. In 2014, Jaremko *et al.* determined the three-dimensional high-resolution structure of mouse TSPO (mTSPO) in complex with its high-affinity ligand (*R*)-PK11195 (Fig. 1) by means of NMR spectroscopy [5, 6]. In the structure of the complex, PK11195 is strongly bound to a hydrophobic cleft within the helical bundle. When complexed with PK11195, the structure of mTSPO appears very rigid; however, by contrast, mTSPO showed conformational flexibility when the same analysis was performed in the absence of a high-affinity ligand [7]. Soon after this study, crystal structures of TSPO homologues from two bacteria, *Rhodobacter sphaeroides* (*Rs*TSPO) [8] and *Bacillus cereus* (*Bc*TSPO) [9], were resolved by X-ray crystallography. They confirmed that monomeric TSPO produces dimers in the membrane, with each monomer composed of 5 TM helices.

TSPO plays a pivotal role in the rate-limiting step of steroidogenesis, namely the translocation of cholesterol across the outer to the inner mitochondrial membrane. Here, cholesterol is converted by the cytochrome P450 side-chain cleavage enzyme (P450ssc) into pregnenolone, which is the first precursor for all neurosteroids and which exerts potent antidepressant, anxiolytic, sedative, anticonvulsant, amnesic, and analgesic effects, mostly by positively modulating the γ-aminobutyric acid type A receptor ($GABA_AR$) in an allosteric manner. Furthermore, the generated neurosteroids exert neurotrophic, neuroprotective, antiapoptotic, and anti-inflammatory activities in several animal models of cerebral ischemia, traumatic brain and spinal cord injury, peripheral neuropathy, and neurodegenerative pathologies [10-12]. In addition, TSPO takes part in a wide breadth of physiological processes such as immunomodulation, mitochondrial metabolism and function, apoptosis induction, cell respiration, and oxidative processes, cell growth and differentiation, and regulation of immune functions [13-16].

Under physiological conditions, TSPO is widely distributed among most peripheral organs including the heart, kidney, lungs, nasal epithelium, and adrenal glands with the highest concentration in steroid-producing tissues. Lower expression is observed in the liver and in resting microglial and neurons of the healthy brain [17].

TSPO expression is altered in a variety of human diseases [18, 19]. In the central nervous system (CNS), TSPO is largely upregulated in microglia cells by inflammatory stimuli. Moreover, reactive astrocytes have been found to overexpress TSPO. High TSPO expression in glial cells is implicated in several neurodegenerative and neuroinflammatory diseases including Parkinson's disease, Huntington's disease, dementia, amyotrophic lateral sclerosis, Alzheimer's disease, multiple sclerosis [20], and some psychiatric disorders [21]. Overexpression of TSPO has been also observed in some neoplastic diseases including breast, colorectal, hepatocellular cancers, as well as glioma and adenocarcinoma. A correlation between TSPO levels and the metastatic potential of human breast cancer and brain gliomas has been supposed. Moreover, alterations in TSPO levels have been observed in patients with generalized anxiety (detected in lymphocytes and platelets), schizophrenia [22], panic, post-traumatic stress [23], and obsessive-compulsive disorders [24]. Changes in TSPO expression have been also observed during ischemia-reperfusion injury [25]. Finally, TSPO might also serve as a potential imaging marker for brown adipose tissue (BAT) mass, because of its distinctly high abundance in mitochondria [26].

Because of TSPO overexpression is associated with several pathological conditions, this protein represents an especially valuable biomarker that could assist diagnosis, predict clinical outcomes, and quantify response to therapeutic interventions for various diseases, in particular neurodegenerative [27-29] and neuropsychiatric disorders [30] but also cancer [31] and inflammatory pathologies [32]. These findings supported considerable efforts toward the design of radioligands for the *in vivo* imaging of TSPO by positron emission tomography (PET).

In this review, we will briefly elucidate concerns with regard to the imaging of TSPO with PET and the basic principles behind the development of adequate radioligands. We will focus on the medicinal chemistry that has led to the design and development of the various TSPO PET radioligands that have appeared in the literature.

2. BINDING OF TSPO LIGANDS AS AN INDIRECT INDEX OF NEURONAL DAMAGE

Because of its non-invasive nature and its ability with suitable radioligands to measure selected proteins at low concentrations, PET can provide quantitative *in vivo* biological information and play an important role in disease diagnosis and progression and in therapy assessment [33].

Molecular imaging by PET may allow detection and quantification of brain inflammatory status and, therefore, may be a useful tool for diagnosis, therapy monitoring, and for the development of novel putative treatments. In this context, TSPO is the prototypical imaging target in neuroinflammation. PET imaging using TSPO as a biomarker has provided important insights into the progression of an expanding list of neurodegenerative and other diseases. However, after almost 4 decades of research, it is recognized that TSPO as inflammatory biomarker has some important limitations. Also, there are some surrounding misperceptions of TSPO pervading the scientific community. Recently, research is focused on the exploration of new targets and tracers for PET imaging of microglial activation.

Other receptors and enzymes are altered during neuroinflammation such as P2X7 receptors, monoamine oxidase-B (MAO-B), cyclooxygenase-2 (COX-2), cannabinoid receptor type 2 (CB2) and tissue transglutaminase (TG2). For these targets, some PET radiotracers have already been developed and evaluated in preclinical and clinical models. Discussion about these emerging targets and the advantages/disadvantages of using specific ligands as PET tracers in neuroinflammatory-based diseases can be found in recent reviews [34-36].

The measurement of neuroinflammation by TSPO PET imaging and reliable correlation with brain pathology is quite complex. *In vitro* experiments, using receptor autoradiography or receptor binding assays, validate TSPO to be a marker of neuroinflammation. The experimental conditions are regulated and maximized to obtain the best signal-to-noise ratio and increases in radioligand binding to TSPO in the regions affected by neuroinflammation are easily detected and compared to the very low levels of TSPO in healthy areas. By contrast, the *in vivo* application of TSPO as a biomarker to quantify inflammation and correlate it with disease progression has raised important warnings that require consideration to avoid misinterpreting PET-imaging results. Firstly, in living animal models or humans, a complex environment composed of different kinetic compartments has to be considered. In addition, critical parameters including blood circulation, permeability through the blood-brain barrier (BBB), metabolism, and excretion need to be considered. Furthermore, TSPO is abundantly expressed in peripheral organs and most of the injected TSPO radioligand will bind in these areas. Although most human studies have demonstrated statistically significant increases of TSPO binding in areas of injury expressing activated glial cells, the amount of signal varies amongst the different neurological diseases and their different stages. Representative results of TSPO PET imaging in inflammatory models or diseases, as well as a detailed discussion of obstacles in the identification of neuroinflammation by use of TSPO PET imaging can be found in recent reviews [34, 36, 37].

3. TSPO RADIOLIGAND PROPERTIES THAT INFLUENCE IMAGE QUALITY IN PET

A crucial aspect of TSPO PET imaging is to establish which radioligand to use. The ideal PET radioligand has to fulfill criteria other than those that apply to drug molecules, and different aspects have to be considered when developing lead compounds into either drugs or PET ligands. The prototypical radioligand [^{11}C](*R*)-PK11195 (Fig. 1), developed as its racemate in 1984, is still the most widely used PET radioligand to localize TSPO and visualize changes in its expression level changes *in vivo*. Nevertheless, this radioligand has several limitations that have encouraged the search for better ones. Several new classes of ligands have been developed but, unfortunately, to date no one radioligand meets all requirements to be ideal for imaging TSPO. This section discusses the main issues to be considered in the design of a TSPO PET ligand, while the different compound classes and their members will be reviewed in the subsequent section.

3.1. Affinity and Selectivity

In general, for PET ligands, high affinity is particularly crucial for obtaining a target-specific signal. TSPO in the brain is expressed at very low levels, and it is mandatory

for a radioligand to show a very high affinity in the low nanomolar to the subnanomolar range. In fact, the required affinity for a successful PET ligand is related to the maximum concentration of available target binding sites (B_{max}) in a brain region. Therefore, the lower the expression level, the higher the affinity required for a radioligand to show *in vivo* specific binding. It has been suggested that an adequate radioligand should have an *in vivo* B_{max}/K_d value greater than ten [38], even if there are some notable exceptions. Similarly, high selectivity for TSPO is essential to avoid specific interactions with other targets. Moreover, the selectivity required for the radioligand is related to the level of expression and distribution of TSPO across brain regions.

In contrast to bioactive drugs, high-affinity TSPO radioligands usually need to be administered in low microgram or sub-microgram amounts to avoid saturating target binding sites with the non-radioactive ligand. Compliance with the 'tracer principle', namely lack of perturbation of the biological system by the radioligand, must also be ensured by low mass injection.

3.2. Lipophilicity

In the design of a TSPO radioligand, the lipophilicity of the molecule has to be taken into major consideration, as it will influence the extent of nonspecific binding and the ability to cross the BBB. Nonspecific binding results from the ability of a compound to bind without specific or saturable interactions with membranes, proteins, lipids, or other cell components.

Undesirable lipophilicity is one of the main factors why a high-affinity radioligand may have major limitations for PET imaging. In fact, lipophilicity is one of the main features that make [^{11}C](*R*)-PK11195 an inadequate TSPO radioligand. In practice, nonspecific binding may be evaluated in a TSPO blocking experiment and is often found to correlate with radioligand lipophilicity [39, 40]. Conversely, lipophilicity strongly influences the ability of a compound to penetrate the BBB. Like all small druglike molecules, PET ligands usually exploit only passive diffusion to cross the lipid bilayer of the BBB from plasma into the brain. As predicted by Lipinski's Rule-of-Five and Jorgensen's Rule-of-Three, passive diffusion is favored for compounds with a molecular weight below 500 Da and having suitable lipophilicity. Therefore, while very high ligand lipophilicity induces excessive nonspecific binding, low lipophilicity reduces BBB permeability. The log*D* value at physiological pH of 7.4 for a brain PET radioligand should be in the range of 1 to 4 with the optimal value of log*D* being around 2.2 [41]. It is worth mentioning that there are other important physical and chemical properties that influence brain entry; for example, some compounds may be recognized by one or more efflux transporters that decrease brain uptake. All these issues should be considered in the design of a PET radioligand [42-44]. Prediction models to define the optimal physical and chemical properties for radioligand design are now available [45].

3.3. Appropriate Radionuclide

Two radionuclides that are commonly used to label TSPO PET radioligands are carbon-11 (^{11}C) and fluorine-18 (^{18}F). The main appeal of ^{18}F is its longer half-life ($t_{1/2}$ = 109.8 min) relative to that of ^{11}C ($t_{1/2}$ = 20.4 min). This may permit commercial radioligand distribution

of ^{18}F-labeled ligands to clinical PET centers that lack radiochemistry facilities. In addition, fluorine-18 can give PET images with somewhat higher spatial resolution than carbon-11 due to its lower positron energy, although this is rarely a major consideration [46-47]. Short-lived carbon-11 cannot be transported to remote facilities and the final radiotracer has to be in close proximity to the site of synthesis. However, an advantage of carbon-11 for local use is that one subject may be injected more than once on the same day with the same radioligand, where injections are separated by a period allowing almost full radioactive decay after the first injection (*i.e.* 10 half-lives or 3.3 hours). This can be convenient to obtain a baseline experiment followed by an experiment in which some pharmacological or other challenge is made on the same subject. In general, the fast decay of carbon-11 means that the radiation burden on the subject is well within approved limits [48].

Whereas fluorine atoms are not common constituents of biomolecules, carbon is ubiquitously present and the isotopic replacement of natural abundance carbon with ^{11}C does not affect the physicochemical and biochemical properties of the molecule. As will be explained in detail below, almost all TSPO radioligands developed so far have a tertiary *N*-methyl amido position that is usually readily labeled by ^{11}C-methylation. Even if fluorine is usually absent in a TSPO ligand, in many ligands fluorine might be inserted at a hydrogen position which is one of the most common bioisosteric replacements in medicinal chemistry [49]. The replacement of hydrogen for fluorine in an organic molecule induces only minimal steric perturbation as the van der Waal's radii of fluorine and hydrogen are similar (1.35 and 1.20 Å, respectively), but more significantly increase molecular weight. The strong electron-withdrawing property of fluorine is reflected in the dipole moment of the carbon-fluorine bond and this could alter the electronic properties of the molecule and consequently the biological behavior. The replacement of a hydrogen atom with fluorine would be expected to modestly increase the lipophilicity of a molecule based on the π coefficient of 0.14 determined for fluorine [50, 51]. However, fluorination of a molecule does not necessarily lead to an increase in lipophilicity and this bioisosteric substitution reduces the overall lipophilicity in some structural environments. Therefore, labeling with fluorine-18 usually results in modification of the physicochemical properties and biological activity of known ligands. In addition, the exchange of hydrogen by fluorine is a well--validated approach in medicinal chemistry to modulate metabolism, because the electron-withdrawing properties of fluorine and the high strength of the carbon-fluorine bond render the latter chemically resistant under most biological conditions. Nevertheless, almost all PET radioligands undergo appreciable metabolism over the time course of a PET scan, sometimes generating radiometabolites that are able to cross the BBB and affect brain radioligand quantification. It is to be pointed out that ^{18}F-labeled ligands may be subject to peripheral radiodefluorination resulting in [^{18}F]fluoride ion in plasma that will be taken up in bone. If the radioactivity in the skull becomes appreciable, the accurate measurement of radioactivity in brain regions near the skull, such as in the neocortex, will be markedly compromised. Although it is not possible to anticipate the susceptibility of an ^{18}F-labeled compound to be radiodefluorinated in human subjects, in general, fluorine-18 atoms bound to carbons in benzene or pyridine rings are generally expected to show strong resistance to metabolic defluorination. It is well known that radioligands labeled with fluorine-18 in an aryl methoxy group are susceptible to radiodefluorination, while fluorine-18 present at the

terminus of a straight saturated alkyl chain of two or more carbons is usually more resistant to defluorination in human subjects.

In TSPO radioligand development, the preparation of ^{18}F-labeled ligands is often concomitant with the synthesis of ^{11}C-labeled analogues. Fluorine-18 is frequently inserted at a benzene ring, in an *N*-methyl or *N*-ethyl position, or at the end of an aryl fluoroalkoxy groups. A discussion of the common methods for the incorporation of carbon-11 or fluorine-18 into small organic compounds such as TSPO ligands is outside the scope of this review, but a summary of common methods may be found in reference [41].

3.4. Metabolism and Site of Labeling

In the design of any brain radioligand, the selection of the molecular position for the label needs to be carefully considered. The easiest and most obvious way of labeling a molecule may not be the optimal solution, because the metabolism of the PET ligand needs to be considered. Since PET cannot discriminate between signals from different radioactive compounds, one or more radiometabolites might severely compromise the outcome measures from PET experiments. Therefore, in the preliminary evaluation of the value of a putative TSPO radioligand, it is essential as far as possible to verify that the radiometabolites that are formed during data acquisition do not harm the PET signal.

PET ligands should not undergo any significant metabolism within the brain and should not be metabolized excessively fast in the periphery during the PET scan. Notwithstanding, peripheral metabolism of a radioligand without generation of radiometabolites that enter the brain can be beneficial in clearing radioligand from plasma and hence also for clearing nonspecific binding from the brain because of the rapid dynamic equilibrium of free radioligand that will exist between plasma and brain.

Lowering the nonspecific binding increases the signal-to-noise ratio (binding potential, *BP*). If the metabolism occurs only in the periphery and not within the brain, an effective strategy for avoiding radiometabolite entry into the brain is to judiciously position the site of labeling. If the metabolism yields radiometabolites with high lipophilicity, they might be able to cross the BBB and thereby add to the combined PET image with the parent radioligand. On the other hand, if radioligand metabolism produces only hydrophilic radiometabolites that are not able to enter the CNS, there is likely no contamination of the final images [43]. Therefore, in the development of PET radioligands, it is not unusual to design and synthesize radioligands that differ only in the molecular position of the radiolabel. This strategy may not only result in better radioligands but may also allow a useful test of whether radiometabolites contaminate the PET signal. If changing the site of labeling in the same ligand furnishes identical signals, it is very likely that there is no contamination by radiometabolites; if the outcomes are different, the presence of radiometabolites is an issue for at least one version of the radioligand [41]. Further evidence of whether radiometabolites contaminate the signal in the brain can be obtained by assessing the stability of the measured volume of distribution (V_T), (or preferably after correction of this parameter for the free fraction of radioligand in plasma f_P)), over the period of data acquisition during a PET scan at baseline. V_T increases with an increase in specific binding and is an important output measure from a baseline scan. V_T is composed of the sum of the

volume of distribution of specific binding (V_S) and the volume of distribution of nonspecific binding (V_{ND}). Ingress of radiometabolites into the brain will likely increase V_{ND} and therefore V_T. Values of V_T/f_P (or V_T) that show time instability suggest radiometabolite contamination in the brain.

3.5. Single Nucleotide Polymorphism in the TSPO Gene

In 2008, during the development of [^{11}C]PBR28 (see Section 4.3), clinical PET studies that were aimed at evaluating the ability of this new ligand to quantify TSPO in the human brain revealed that a small percentage (~14%) of healthy subjects presented no significant specific binding of [^{11}C]PBR28 in the brain and peripheral organs. This was a remarkable finding because non-binding to TSPO had never been reported with [^{11}C](*R*)-PK11195, despite its use for decades [52]. The reason for this finding was not initially understood and various hypotheses were considered. Nevertheless, this observation paved the way for one of the most important discoveries in the TSPO radioligand field, the influence of a single nucleotide polymorphism (SNP) in the TSPO gene. Later studies revealed similar findings for other TSPO radioligands. Together, these findings suggested the existence of three different human subject categories, now called high-affinity binders (HABs), low-affinity binders (LABs), and mixed-affinity binders (MABs) [44, 53]. It was then demonstrated that the TSPO binding affinity category correlates with the presence of a SNP (rs6971) in the TSPO gene that leads to an amino acid substitution (Ala147Thr, A147T). HABs are homozygous for wild-type TSPO, whereas MABs are heterozygous, and LABs are homozygous for the Ala147Thr TSPO [54]. Thus, individuals with the same TSPO density but different genotypes will produce different PET signals. Crystal structures of TSPO from *Rhodobacter sphaeroides* and a mutant that mimics the human A147T polymorphism suggested that this substitution alters the structure of TSPO, including decreasing the distance between the second and fifth transmembrane domains and that this change in conformation impacts the binding of almost all reported TSPO ligands, which bind the mutant TSPO with lower affinity [8]. The relevance of the SNP rs6971 in TSPO to the interpretation of clinical PET data is evident. Although each radioligand has a unique level of sensitivity, as depicted in the next section, studies with TSPO radioligands must take SNP rs6971 into account by doing TSPO genotyping before imaging. This task is an unwelcome extra burden in any PET study. Often LABs must be excluded because the brain has too little uptake to quantify and studies that include HABs and MABs need a suitable correction for binding levels across genetic groups [55]. It is not surprising, therefore, that recent efforts in TSPO radioligand design have focused on the development of ligands with low SNP rs6971 sensitivity.

4. CHEMICAL CLASSES OF TSPO RADIOLIGANDS

To date, several dozen TSPO radioligands have been synthesized and have undergone preclinical or clinical evaluation to image the expression of TSPO, principally in the brain. Considering the aforementioned properties, TSPO radioligands are conventionally classified into three generations. First-generation TSPO PET radioligands include only the benzodiazepine [^{11}C]Ro5-4864 (Section 4.1, Fig. 2 and, above all, the isoquinoline carboxamide [^{11}C](*R*)-PK11195 (Section 4.2, Fig. 1). Even if the latter is still the most

widely used PET radioligand to localize TSPO and visualize its expression level changes *in vivo*, [^{11}C](*R*)-PK11195 has a relatively moderate receptor affinity, is highly lipophilic, and has a low brain uptake. Second-generation TSPO PET radioligands comprise almost all those developed to circumvent the limitations of [^{11}C](*R*)-PK11195. They have arisen from different structural classes, feature higher affinity and lower lipophilicity, and therefore have improved TSPO specific signals and superior imaging characteristics compared to [^{11}C](*R*)-PK11195. However, unlike [^{11}C](*R*)-PK11195, the second-generation radioligands suffer from sensitivity to SNP rs6971, with the ratio of affinity for the two alleles varying considerably across different radioligands. Third -generation TSPO radioligands were developed with the aim to combine the high TSPO specific signals of second-generation ligands and the low sensitivity to SNP of [^{11}C](*R*)-PK11195. To date, only two compounds, namely [^{18}F]GE180 (Section 4.5) and [^{11}C]ER176 (Section 4.2), are included as lowly rs6971 sensitive third-generation TSPO PET ligands.

TSPO radioligands will be described in detail in this section. Table 1 summarizes the chemical classes of TSPO radioligands, representative compounds, and the leading properties to be considered in the early stages of development.

Although these compounds belong to different chemical classes, almost all share common structural characteristics. Indeed, they exhibit a central aromatic planar core featuring an acetamide function, which is a crucial requirement for efficient binding to the receptor. In addition, the central planar skeleton is directly linked to an aromatic ring [56].

4.1. Benzodiazepines

The benzodiazepine Ro5-4864 (Fig. 2) has a nanomolar affinity for TSPO and a 1000-fold lower affinity for central benzodiazepine receptors and was the first compound reported as a specific TSPO ligand. Therefore, it was speculated that radiolabeled derivatives could be useful tools for nuclear imaging of neuroinflammation. However, early PET studies performed with [^{11}C]Ro5-4864 in human subjects with gliomas failed to demonstrate higher radioactivity levels in gliomas than in healthy brain regions. Similar disappointing results were obtained *in vitro*; [^{11}C]Ro5-4864 exhibited little binding in surgically removed samples of human gliomas [57]. These poor results could be ascribed to different reasons, such as nonspecific lipophilic and electrostatic interactions between the radioligand and brain tissue and a species-dependent binding [58]. Substitution of iodine for chlorine at either the 7- or 4'- position of Ro5-4864 resulted in only a small decrease in binding affinity for TSPO. Thus, an iodo-ana-log of Ro5-4864 was radiolabeled to yield a potential SPECT ligand [59]. *In vivo* binding of [^{125}I]Ro5-4864 to TSPO located in C6 glioma tissue was used to image the tumor by autoradiography. However, no successful SPECT imaging was reported. The limitations of benzodiazepines as tools for TSPO PET imaging and the concomitant discovery of the isoquinolinecarboxamide class as more effective TSPO ligands, have rendered this class of compounds unworthy of further development.

4.2. 3-Isoquinolinecarboxamides, Quinoline-2-Carboxamides, and Quinazolines

The 3-isoquinolinecarboxamide [^{11}C]PK11195 (Fig. 1) was synthesized in the same year as [^{11}C]Ro5-4864 [60] and immediately shown to be superior. Indeed, [^{11}C]PK11195

displayed higher overall uptake and higher specific binding in gliomas than [^{11}C]Ro5-4864 [57]. Initially used as a racemate (K = 9.3 nM), further *in vivo* studies revealed that the (*R*)-e-nantiomer was retained to a significantly greater extent than the (*S*)-enantiomer in sites enriched in TSPO binding sites. These results agreed with *in vitro* binding experiments that showed that the (*R*)-enantiomer has 2--fold greater affinity for TSPO binding (K_i = 2.9 nM, human) than the (*S*)-enantiomer [61]. [^{11}C](*R*)-PK11195 represents the prototypical first-generation TSPO radioligand and has been used for decades to image TSPO in neurological and psychiatric disorders. Even if [^{11}C](*R*)-PK11195 is in several aspects inferior to newer radioligands, it has still been widely used in clinical trials to assess the role of activated microglia in cognitive impairment [62], amyotrophic lateral sclerosis [63], psychosis [64], fibromyalgia and complex regional pain syndrome [65], Creutzfeldt-Jakob disease [66] and other neurodegenerative disorders. However, [^{11}C](*R*)-PK11195 suffers from critical limitations that reduce its value as a PET imaging agent. One of the main concerns is its high lipophilicity (logD_{74} = 3.97), which leads to a high level of nonspecific binding. This, in combination with its only moderately high affinity, results in a poor signal-to-noise ratio and low specificity in PET imaging. Other issues are high plasma protein binding and low brain permeability, which further complicate its accurate quantification [67, 68]. For these reasons, the reduced ability to detect subtle changes in TSPO density makes [^{11}C](*R*)-PK11195 unsuitable for nuclear imaging in some diseases [69]. Despite these limitations, [^{11}C](*R*)-PK11195 shows remarkably low sensitivity to SNP rs6971 *in vitro*, although it may have some sensitivity *in vivo* [44].

An analogue of PK11195 with the longer-lived fluorine-18 label has been prepared, namely [^{18}F]PK14105, (Fig. 3). This radioligand showed a slight decrease in binding affinity with respect to PK11195 *in vitro* and no advantages in preliminary studies *in vivo* [70, 71].

Several quinoline-2-carboxamides have been designed as conformationally restrained analogues of PK11195 (Fig. 4). The highest affinity representatives of this class, VC193M (IC_{50} = 2.1 nM), VC198M (IC_{50} = 2.9 nM), and VC195M (IC_{50} = 2.1 nM), were labeled with carbon-11 to assess their potential for TSPO imaging [72]. At first, they were evaluated for imaging microglia activation in neurodegenerative processes [73]. Only [^{11}C]VC195 gave results comparable to those obtained with [^{11}C](*R*)-PK11195. The fluoromethyl derivative [^{11}C]VC701 showed an IC_{50} value of 0.11 nM corresponding to about 20 times more potency than PK11195. Biodistribution experiments in animals showed higher tissue-to-plasma ratios for [^{11}C]VC701 than for [^{11}C]VC195, suggesting a lower interaction of this compound with plasma proteins [74]. Moreover, VC701 was labeled with fluorine-18 for evaluation of its kinetics and pharmacologic properties in animals. VC701 was found to be a specific TSPO ligand [75]. However, no studies on the sensitivity of [^{18}F]VC701 to SNP rs6971 have been reported.

With the aim to improve the signal-to-noise ratio of [^{11}C](*R*)-PK11195, several 4-phenylquinazoline-2-carboxamides were designed as TSPO ligand azaisosteres of PK11195. The replacement of one carbon in the central planar core by a nitrogen atom was anticipated to confer better druglike character, because of higher hydrophilicity and water solubility than their quite lipophilic isoquinoline counterpart [76, 77]. Some of these new ligands were labeled with carbon-11 and evaluated as candidate PET ligands for imaging brain

TSPO. [^{11}C]ER176 (Fig. 5), the direct 4-azaisostere of [^{11}C](*R*)-PK11195, was particularly promising because it offers many radioligand properties that are superior to those of the parent compound. Indeed, [^{11}C]ER176 was found to have higher binding affinity (rat K_i = 3.1 *versus* 9.3 nM) and lower lipophilicity (log$D_{7.4}$ = 3.55 *versus* 3.97) than [^{11}C](*R*)-PK11195. Moreover, [^{11}C]ER176 exhibited excellent brain kinetics and high TSPO specific signal in PET studies of monkey [78] and human brains [79]. Remarkably, [^{11}C]ER176 shows low *in vitro* sensitivity to SNP rs6971 as its ratio of binding affinity in HABs to that in LABs was only 1.3 to 1, a ratio comparable to that of [^{11}C](*R*)-PK11195. Even if it displays some sensitivity to SNP rs6971 *in vivo*, [^{11}C]ER176 still nevertheless allows quantitation in LABs and gives high binding potentials for all genotypes compared to second-generation radioligands [80]. This allows individuals with all TSPO polymorphisms to be included in PET imaging studies, although binding measurements must still be corrected for genotype. A study comparing four ^{11}C-labeled TSPO radioligands, [^{11}C](*R*)-PK11195, [^{11}C]PBR28, [^{11}C]DPA713, and [^{11}C]ER176, confirmed that [^{11}C]ER176 had a high signal-to-noise ratio and was least likely to generate radiometabolite that could penetrate BBB [81]. For these reasons, [^{11}C]ER176 is, at present, considered the first third-generation TSPO ligand and is regarded as the best performing radioligand for imaging and quantifying TSPO [34, 82]. A preferred method for producing this radioligand for human studies in a CGMP level laboratory has recently been described in detail [83].

Recently efforts have been made to develop an ^{18}F-labeled version of ER176. Six potential candidates, comprising the *o*-, *m*-, and *p*- fluoro and trifluoromethyl deschloro-phenyl analogues of ER176, were prepared and labeled in the *N*-methyl group with carbon-11. All six radioligands have high TSPO affinity, acceptable lipophilicity, and quite a low genotype sensitivity *in vitro*. They performed well in mice, with the *m*-fluoro ligand concluded to be marginally superior on the basis of the estimate of the ratio of TSPO specific to nonspecific binding in mouse brain, which was comparable to that from [^{11}C]ER176. This ligand, dubbed FS51 (Fig. 5), was labeled with ^{18}F and gave similar results to the ^{11}C version in mice [84]. [^{18}F]F-S51 (rat kidney K_i = 5.17 nM; log$D$ = 3.09) warrants further evaluation in higher species.

4.3. Phenoxyarylacetamides

The formal opening of the azepine ring of Ro5-4864 resulted in phenoxyphenylacetamides as TSPO ligands (Fig. 6). They generally feature high affinity and specificity. The first ^{11}C-labeled representative of this class was [^{11}C]DAA1106 [85, 86]. This displayed high affinity for TSPO in mitochondrial fractions of rat (K_i = 0.043 nM) and monkey (K_i = 0.188 nM) brains and acceptable lipophilicity (log$D$ = 3.65). After intravenous injection into mice, [^{11}C]DAA1106 accumulates in high TSPO density brain regions. In rat models of neuroinflammation [^{11}C]DAA1106 binds to microglia with higher affinity than [^{11}C](*R*)-PK11195 [87]. Several studies confirmed that this second-generation radioligand may be reliable for PET scanning *in vivo* [88]. In a study to quantify TSPO receptors in patients with Alzheimer's disease, [^{11}C]DAA1106 showed increased uptake in multiple brain regions in patients versus age-matched healthy controls [89]. Moreover, [^{11}C]DAA1106 has been used in PET studies in patients with chronic schizophrenia to verify the involvement of the glial reaction process in the pathophysiology of the disease [90] and, recently, in healthy

volunteers to confirm that smokers have impaired inflammatory functioning compared with nonsmokers. That is smokers have less radioligand binding than non-smokers [91, 92].

Along with the development of [^{11}C]DAA1106, [^{18}F]DAA1106 and other ^{18}F-labeled analogues were also synthesized and evaluated. [^{18}F]FMDAA1106 was obtained by the bioisosteric replacement of hydrogen by fluorine in the methoxy group of the parent compound and [^{18}F]FEDAA1106 was designed by homologation (lengthening the methoxy chain by CH_2) of [^{18}F]FMDAA1106 [93]. As anticipated, [^{18}F] FMDAA1106 displayed binding affinity similar to the parent compound, while substituting the OCH_3 group with OCH_2CH_2F was favorable; the K_1 value (0.078 nM) of [^{18}F]FEDAA1106 was 2-fold higher than that of [^{11}C]DAA1106, and 10-fold higher than that of [^{11}C]PK11195. However, [^{18}F]FMDAA1106 was rapidly metabolized by defluorination in mouse plasma and brain. The PET image of this radioligand in the monkey brain also showed radioactivity in the bone, indicating that it was not a useful PET ligand because of defluorination *in vivo*. By contrast, its superior homologue [^{18}F]FEDAA1106 was metabolized in the mouse by debenzylation to a polar radiometabolite in the plasma and no radiometabolites were detected in the brain. [^{18}F]FEDAA1106 displayed a high uptake in the monkey brain, especially in the occipital cortex, with a radioactivity level 1.5 times higher than that of [^{11}C]DAA1106 [94]. A quantitative analysis of [^{18}F]FEDAA1106 binding to TSPO in human brain has been reported [95], but a study in control subjects and Alzheimer's disease patients indicated that TSPO imaging with this radioligand does not enable the detection of microglial activation in this neurodegenerative disease [96]. With the aim to further reduce metabolism and defluorination, the position of the label was completely changed and the [^{18}F]*N*-fluoroacetyl derivative [^{18}F]PBR06 (also known as [^{18}F]FBR) was prepared and evaluated as a PET radioligand [97]. PBR06 showed higher binding affinity than PK11195 but with interspecies variability; the affinity for human tissue was somewhat lower (K_i = 1.0 nM) than for monkey (K_i = 0.32 nM) and rat (K_i = 0.18 nM). Moreover, it has high lipophilicity (log$D$ = 4.01) which may improve brain penetration but increase nonspecific binding. Nevertheless, in the monkey brain, the specific binding of [^{18}F]PBR06 was greater than 90% of its total uptake. Biodistribution data in humans showed that this radioligand had negligible defluorination. High levels of radioactivity were observed in organs of metabolism and excretion, such as the liver and gallbladder. These relatively high doses to organs of metabolism and excretion must be considered in the clinical use of this radioligand [98, 99]. Nevertheless, [^{18}F]PBR06 has been widely studied in many neurological disease models, such as Huntington’s disease [100] and stroke-associated neuroinflammation [101].

On the basis of the classical bioisosteric equivalence of phenyl and pyridinyl groups, phenoxypyridinylacetamides have also been developed as less lipophilic derivatives of phenoxyphenylacetamides (Fig. 7). [^{11}C]PBR28 exhibited high affinity for TSPO in rat (K_i = 0.68 nM), monkey (K_i = 0.94 nM), and human (K_i = 2.5 nM) mitochondria and, as expected by carbon-nitrogen replacement, showed lower lipophilicity (clog$D$ = 2.95) than [^{11}C]DAA1106 (clog$D$ = 4.28) [102]. Brain and whole-body imaging in monkeys showed that [^{11}C]PBR28 had high levels of specific binding in the brain, about 80-fold higher than that of [^{11}C](*R*)-PK11195 [44, 103]. This radioligand has been used in humans to study disease progression in several disorders that involve microglia activation, such as Alzheimer's disease [104, 105], multiple sclerosis [106], autism spectrum disorders [107],

Huntington's disease [108], rheumatoid arthritis [109] and others. [^{11}C]PBR28 was also used to compare brain TSPO levels in tobacco smokers and non-smokers [110]. However, several studies proved that [^{11}C]PBR28, compared with other second-generation ligands, is very sensitive to SNP rs6971 [111]. Indeed, the differences in affinity between HABs and LABs are about 50-fold with [^{11}C]PBR28, and greater than about 17-fold with [^{18}F] PBR06, and 4-fold with [^{11}C]DAA1106. Therefore, all clinical studies performed with this radioligand without determination of genetic polymorphism must be considered with very high caution [54].

[^{18}F]FMPBR28 is the fluoromethyl derivative of [^{11}C]PBR28. As expected from the bioisosteric replacement of fluorine for hydrogen in the methoxy group, its binding affinity, measured in human leukocyte membranes, is similar to that of PBR28 (IC_{50} = 8.28 nM *versus* 8.07 nM). The two compounds also exhibited comparable lipophilicity (log$D$ = 2.85 *versus* 2.82). Although these two radioligands have almost identical TSPO affinities *in vitro*, they exhibit different pharmacokinetic profiles. In a rat model of neuroinflammation, [^{18}F]FMPBR28 performed better than [^{11}C]PBR28 [112]. However, in a rat model of experimental autoimmune myocarditis, [^{18}w, [^{18}F]CB251 (Section 4.4) provided a more specific TSPO uptake in the inflammatory heart [113].

The replacement of the fluoromethyl moiety in [^{18}F]FMPBR28 with fluoroethyl, gave [^{18}F]FEPPA, a phenoxypyridinylacetamide radiofluorinated ligand that has a somewhat higher affinity for TSPO (K_i = 0.07 nM) than either [^{18}F]FMPBR28 or [^{11}C]PBR28, reduced metabolism, and greater brain penetration in rats than the parent inferior homologue [114]. Quantification of TSPO binding in the human brain showed [^{18}F]FEPPA to be a promising PET ligand to measure neuroinflammation in the human brain [115], but, as expected, it was very sensitive to polymorphism [116]. [^{18}F]FEPPA has been exploited to evaluate the role of neuroinflammation in patients affected by neurodegenerative diseases or psychiatric disorders such as Parkinson’s disease [117], Alzheimer’s disease [118], schizophrenia, and psychosis [119]. Another ^{18}F-labeled phenoxypyridinylacetamide, [^{18}F]6F-PBR28 has been prepared and evaluated as a putative radioligand, but it has not been further investigated [120].

4.4. Nitrogen-containing Bicyclic Compounds: Imidazopyridines and Bioisosteric Structures

These ligands share with quinazolinecarboxamides a few common structural characteristics such as the nitrogen-containing heterocyclic core linked to an acetamide function and an aromatic ring. The first radiolabeled molecules of this class were the imidazo[1,2-*a*]pyridines (Fig. 8). Their design was inspired by the structure of alpidem, a compound that binds both TSPO and central benzodiazepine receptors. [^{11}C]CLINME represents the first radioligand of this class to be labeled with carbon-11. [^{11}C]CLINME compares favorably with [^{11}C](*R*)-PK11195 in PET imaging of rodents with induced local acute neuroinflammation, exhibiting a higher contrast between the TSPO expressing lesion site and the intact side [121]. Structurally related derivatives were labeled with iodine-123 for use in SPECT imaging and *in vitro* pharmacological studies [122]. [^{11}C]PBR170 [123] and [^{11}C]CB148 [124] are other representative examples of ^{11}C-labeled imidazopyridines.

[^{11}C]CB148 shows higher binding affinity (K_i = 0.20 nM) than [^{n}C](*R*)-PK11195 (K_i = 4.26 nM) and distribution studies in mice show its accumulation in TSPO rich regions of the brain. Further studies have focused on structurally related fluoroethyl and fluoropropoxy derivatives that could be labeled with longer-lived fluorine-18. Compounds [^{18}F]PBR102, [^{18}F]PBR111 [125], and [^{18}F]CB251 [126] show nanomolar inhibition constants for TSPO, high selectivity and improved signal-to-noise ratio relative to [^{11}C](*R*)-PK11195. [^{18}F]PBR111 appears to be the most promising radiofluorinated ligand of this class; it has a good binding affinity (K_i = 3.7 nM) and adequate lipophilicity (log*P* = 3.2), showing a better pharmacological profile for brain imaging TSPO expression in neurodegenerative disorders [127]. [^{18}F]PBR111 has been used in several preclinical experiments and evaluated in clinical studies [128]. However, the SNP rs6971 has a strong effect on the binding affinity of [^{18}F]PBR111 to TSPO in human tissue *in vitro* and this result was confirmed in studies on healthy humans, as appreciable differences were observed between HABs, MABs, and LABs [129]. Recent studies tested the selectivity of [^{18}F]CB251 to SNP rs6971. *In vitro* experiments demonstrated that this radioligand has high binding affinity (K_i = 0.27 nM), adequate lipophilicity (log*D* = 3.00) coupled with a lower genotype sensitivity (ratio of LAB/HAB IC_{50} = 1.14) than other TSPO radioligands [130]. However, [^{18}F]CB251 still showed different uptakes in HABs and LABs in human PET studies, as previously reported for [^{11}C]ER176. This radioligand needs further evaluation.

Pyrazolo[1,5-*a*]pyrimidine ligands were derived by bioisosteric nitrogen for carbon replacement in the imidazopyridine class (Fig. 9). The first compounds developed were [^{11}C]DPA713 (K_i = 4.7 nM) [131] and [^{18}F]DPA714 (K_i = 7.0 nM) [132] which specifically localize neuroinflammatory sites *in vitro* with a similar signal-to-noise ratio. Both have the same log*D* value (2.44), which is lower than that of PK11195 (3.35). In a rodent model of ischemic stroke, [^{11}C]DPA713 performed better than [^{18}F]GE180 (Section 4.5) in the identification of acute and chronic inflammation in infarcted brain tissue [133]. In the human brain, [^{11}C] DPA713 showed a signal-to-noise ratio 10 times higher than that of [^{11}C](*R*)-PK11195 in HABs. However, [^{11}C]DPA713 showed sensitivity to SNP rs6971 in the brain, and LABs needed to be excluded from clinical studies. Moreover, there was evidence of radiometabolite accumulation in the brain [134].

The fluoro derivative [^{18}F]DPA714 seems to be the most promising in the pyrazolopyrimidine class of TSPO radioligands. In an *in vivo* rat model of acute neuroinflammation, [^{18}F]DPA714 performed better than [^{11}C]DPA713 and [^{11}C](*R*)-PK11195, with the highest ratio of ipsilateral to contralateral uptake and the highest binding potential [135]. [^{18}F]DPA714 has recently been used as a TSPO radioligand for neuroinflammation. For instance, *in vitro* autoradiography experiments assessing radioligand binding specificity showed a strong relationship between [^{18}F]DPA714 uptake and activation level of glioma-associated myeloid cells [136]. [^{18}F]DPA714 was successfully used in a mouse model of human orthotopic glioma to identify specific reactive areas of myeloid cell infiltration in the tumor microenvironment [137]. In humans, [^{18}F] DPA714 has been used to image neuroinflammation in patients with Alzheimer's disease [138] and multiple sclerosis [139]. [^{18}F]DPA714 has also been exploited to monitor BAT activity in tumor-bearing mice *in vivo* [140]. However, [^{18}F]DPA714 also has some drawbacks. As for all second-generation radioligands, genotyping of subjects is a prerequisite for quantification of

[^{18}F]DPA714 PET images [141]. In addition, [^{18}F] DPA714 shows defluorination as primary metabolism *in vivo* [142].

To improve on the instability of [^{18}F]DPA714 towards radiodefluorination, [^{18}F]FDPA was prepared. In this derivative, the ethoxy linker between the label and the aromatic ring was removed and the ^{18}F was placed directly on the aromatic ring, a position that is expected to be resistant to defluorination [143]. [^{18}F]FDPA showed a good TSPO binding affinity (K_i 1.7 nM) and in preclinical evaluation demonstrated higher metabolic stability compared to [^{18}F]DPA714 [144]. [^{18}F]FDPA was evaluated in a mouse model of Alzheimer's disease [145, 146].

With the aim to obtain new TSPO radioligands with greater affinity and potentially more robust PET imaging, the pyrazolopyrimidine scaffold of DPA714 was optimized. Specifically, to explore the effects of substituents that varied in steric bulk, a focused library of 5,6,7-substituted pyrazolopyrimidines was developed. These substituents included hydrogen, methyl, ethyl, chloro, and 2-propanone and were cross--matched. SAR analysis revealed an improvement in affinity by replacing methyl with ethyl at 5- and 7- positions of the pyrazolopyrimidine core. Subnanomolar affinity was observed for derivative VUIIS1008 (K_i = 0.18 nM), which represents a major 36-fold enhancement in binding affinity over the parent compound DPA714 (K_i = 9.27 nM). As expected, replacing methyl with ethyl resulted in increased lipophilicity (log$P_{7,5}$ = 2.84 *versus* 2.12), which is still suitable for *in vivo* imaging [147]. In preclinical PET studies in healthy mice and glioma-bearing rats [^{18}F]VUIIS1008 exhibited improved tumor-to-background ratio and higher binding potential in tumors than [^{18}F]DPA714 [148]. On the other hand, in a model of cerebral ischemia in rats, [^{18}F]VUIIS1008 did not exhibit better performance than the parent compound [149].

Increasing the substituent at the 7-position of the pyrazolopyrimidine core to a bulkier *n*-butyl group, yielded derivative VUIIS1018A, which features an exceptionally high binding affinity (IC_{50} = 16.2 pM), 700-fold higher than DPA714. However, the introduction of the longer alkyl chain also increased lipophilicity over that of DPA714 (log$D$ = 3.7 *versus* 2.4), which is slightly outside the optimal value [150]. Nevertheless, in animal models, [^{18}F]VUIIS1018A exhibits lower accumulation in healthy brain, an improved tumor--to-background ratio, and a higher specific to nonspecific binding than [^{18}F]DPA714 and [^{18}F]VUIIS1008 [151].

4.5. Indoles

Indole was found to be a valuable scaffold for the central aromatic planar core to develop potent and selective TSPO ligands. Indeed, as early as 1993, a novel series of 2-arylindole-3-acetamides were published and SAR studies defined the structural features required for high-affinity binding to TSPO [152].

The reduction of structural flexibility of the indole-3-acetamides derivatives yielded 2-phenylindole glyoxylamides as TSPO ligands, which were endowed with nanomolar to the subnanomolar affinity for TSPO and complete selectivity with respect to the central benzodiazepine receptor (Fig. 10) [153, 154]. The N^1-methyl-2-(4'-nitrophenyl)indol-3-yl)glyoxylamide (NMPIGA) displayed high affinity (K_i = 5.7 nM) and acceptable

lipophilicity (clog*P* = 3.95) and was selected and developed as a ^{11}C-labeled probe. After intravenous injection, [^{11}C]NMPIGA readily entered the monkey brain giving a high proportion of reversible specific binding to TSPO. However, this new chemotype showed a certain sensitivity to SNP rs6971, having a different affinity for the three forms of TSPO. In particular, [^{11}C]NMPIGA displayed similarly high affinity for HABs (K_i = 1.57 nM) and MABs (K_i = 1.82 nM) and a lower affinity for LABs (K_i = 9.53 nM) [155].

Taking into account the indole-3-acetamide scaffold, the fusion of the indole moiety with a pyridazyne ring yielded the pyridazino[4,5-*b*]indole-5-acetamides as a new class of potent and selective TSPO ligands (Fig. 11). SSR180575 has proven to be the most promising ligand, with high affinity (K_i = 0.83 nM) and selectivity. Moreover, SSR180575 was found to be able to promote neuronal survival and regeneration in animal models of axotomy and neuropathy, effects that are mediated by local synthesis of neurosteroids [156]. Later, SSR180575 was labeled with carbon-11 and evaluated *in vitro* and *in vivo* in a rodent model of acute neuroinflammation demonstrating high specific TSPO binding. *In vitro* autoradiography and *in vivo* brain PET imaging evidenced a higher uptake of [^{11}C]SSR180575 in the ipsilateral striatum, characterized by an increase of TSPO expression, with respect to the intact tissue of the contralateral one. Also in non-human primates, [^{11}C]SSR180575 displayed encouraging PET imaging properties [157, 158].

Starting from SSR180575, a series of compounds functionalized at N^3-position with groups suitable to be substituted with fluorine-18 was developed. Several compounds were found to be very potent, with K_i values comparable to those of the parent SSR180575. The derivative with a 3-fluoro-2-pyridyl moiety in place of the phenyl ring (FPSSR180575) was selected to be labeled. When evaluated in glioma-bearing male Wistar rats by means of PET imaging, [^{18}F]FPSSR180575 showed higher accumulation in tumor brain tissue with respect to the contralateral, non-tumor brain, leading to excellent imaging contrast between tumor and contralateral tissue [159].

Tetracyclic indole has also proven to be a suitable central scaffold for the development of TSPO ligands [160]. Starting from this pharmacophore, the tricyclic 2,3,4,9-tetrahydro-carbazole-4-carboxamide derivative [^{18}F]GE180 was developed (Fig. 12) [161]. Initially identified and evaluated as a racemate, further studies of the resolved enantiomers revealed that the (*S*)-enantiomer had a higher affinity (K_i = 0.87 nM, rat; K_i = 9.2 nM, human) for TSPO than the (*R*)-enantiomer (K_i = 3.87 nM, rat; K_i = 14.1 nM, human) and higher uptake and specificity for TSPO-rich regions. Furthermore, [^{18}F]GE180 had also been shown to be enantiomerically stable *in vivo*, with no observed conversion of the eutomer to the distomer [162]. This radioligand initially seemed very promising and has been used in several preclinical and clinical studies. In a LPS-induced model of neuroinflammation, [^{18}F]GE180 was able to identify sites of activated microglia in both gray and white matter. A comparison between [^{18}F]GE180 and [^{11}C](*R*)-PK11195 revealed that [^{18}F]GE180 performed significantly better for imaging TSPO associated neuroinflammation due to its improved binding potential and its longer half-life [163]. Similarly, in a preclinical rat model of stroke, [^{18}F]GE180 demonstrated a better signal-to-noise ratio than [^{11}C](*R*)-PK11195 [164]. In another preclinical study of Alzheimer's disease, [^{18}F]GE180 was found to be useful for imaging TSPO expression changes in response to neuroinflammation during

normal aging and in pathogenesis in Alzheimer's disease transgenic mice [165]. First, PET studies in healthy humans evidenced that [^{18}F]GE180 had a low first-pass extraction (about 1%) and gave low total distribution volume (V_T) estimates. More importantly, although [^{18}F]GE180 displays a 15-fold affinity difference between HAB and LAB *in vitro*, in human studies it was shown to be quite insensitive to SNP rs6971 compared to other second-generation TSPO PET tracers in humans and this property led to the informal classification of [^{18}F]GE180 as a third-generation TSPO radioligand [166, 167].

[^{18}F]GE180 was successfully used in patients suffering from relapsing-remitting multiple sclerosis and was able to detect areas of focal microglia/macrophage activation in lesions not associated with the patient's genotype. Indeed, high focal uptake was observed not only in HAB and MAB patients, but also in LAB patients [168]. In addition, [^{18}F]GE180 was used for imaging in patients with glioblastoma and provided remarkably high tumor-to-background contrast, showing high uptake even in areas without contrast enhancement on magnetic resonance imaging [169-171]. A subsequent human study [172], in patients with histologically validated glioma, evidenced a clear association between [^{18}F]GE180 uptake and WHO grades, with the highest uptake in WHO grade IV glioblastoma, in line with previous histopathological studies reporting a correlation between TSPO expression and WHO grade [173].

However, a recent study of head-to-head comparison between [^{18}F]GE180 and [^{11}C]PBR28, established that [^{18}F]GE180 has a low brain penetration from the vascular compartment and a low signal-to-background ratio in diseases where the BBB is not broken [174]. Therefore, even if [^{18}F]GE180 at first has received great enthusiasm, it seems now to be far inferior to the second- and third-generation TSPO ligands. Therefore, several research groups do not advise the use of this radioligand [34, 82, 175].

Recently, the introduction of a benzyl moiety in place of the ethyl substituent in [^{18}F]GE180, yielded the compound [^{18}F]GE387. Also, in this case, the (*S*)-enantiomer has a high affinity for TSPO *in vitro*. This radioligand also shows low sensitivity to SNP rs6971 as its LAB/HAB affinity ratio was determined to be 1.3, and similar to that of [^{11}C](*R*)-PK11195. In addition, PET scans in wild-type healthy rats evidenced the ability of the racemic analogue of [^{18}F]GE-387 to enter the brain [176]. To date, no further studies on the biological evaluation of [^{18}F]GE387 have been reported.

4.6. 8-Oxodihydropurines

8-Oxodihydropurines TSPO ligands have common structural characteristics with previous classes, namely, a nitrogen-containing bicyclic aromatic skeleton, an acetamide function, and an aromatic ring directly attached to their central core (Fig. 13).

AC5216 has a sub-nanomolar affinity for TSPO (K_i = 0.2 nM) and adequate lipophilicity (log*D* = 3.3), as necessary for high uptake and low nonspecific binding in the brain. AC5216 has been labeled with carbon-11 [177]. In studies aimed to image microglial activation triggered by amyloid lesions in mouse models of Alzheimer's disease, [^{11}C]AC5216 enabled PET imaging of glial TSPO with high contrast and performed better than [^{18}F]FEDAA1106 [178]. It is to be noted that the unlabeled AC5216 (XBD-173), also known as emapunil,

is a TSPO ligand able to promote neurosteroid synthesis and decrease inflammation; it has completed phase 2 trials for anxiety disorders treatment [179] and gave promising results in a mouse model of parkinsonism [180]. The binding of AC5216 was significantly affected by SNP rs6971 (ratio of LAB/HAB K_i = 12.5) and this could have important implications for the clinical outcomes of this compound [181].

The binding affinity of [^{11}C]DAC is similar to that of [^{11}C]AC5216. However, it has lower lipophilicity (log$D$ = 3.0 *versus* 3.5) [182]. It has been used to measure the slight TSPO expression elevation in ischemic rat brains [183].

^{18}F-Labeled oxopurine analogues of [^{11}C]AC5216 were also evaluated as radioligands. [^{18}F]FEAC (K_i = 0.5 nM), [^{18}F]FEDAC (K_i = 1.3 nM) and [^{18}F]FAC (K_i = 0.55 nM) showed potent *in vitro* binding affinity for TSPO but lower than the parent compound. In a rat model of neuroinflammation, [^{18}F]FEAC and [^{18}F]FEDAC gave high uptake of radioactivity in a kainic acid-infused striatum, a brain region where TSPO expression was augmented [184]. Investigation of [^{18}F]FEAC and [^{18}F]FEDAC kinetics in the monkey brain and PET imaging of TSPO in the infarcted rat brain showed that each ^{18}F-labeled ligand had uptake and distribution patterns in the monkey brain similar to those of [^{11}C]AC5216. However, after injection into the monkey, the uptake of each ^{18}F-labeled ligand in the brain decreased over time whereas that of [^{11}C]AC5216 did not. The relatively rapid kinetics may be due to the lower binding affinity of both ^{18}F-labeled ligands. As far as metabolism was concerned, the percentage of unmodified radioligand was up to 80% in the brain homogenate of mice 15 min after injection. The monkey plasma metabolite analysis confirmed the adequate stability of [^{18}F]FEAC and [^{18}F]FEDAC [185]. [^{18}F]FEDAC enabled the visualization of active inflammation sites in arthritic joints in a collagen-induced arthritis model by targeting TSPO expression in activated macrophages [186].

4.7. Benzoxazolones

Replacement of the oxodihydropurine core with a benzoxalone scaffold yielded a novel class of TSPO ligands (Fig. 14). The first compound evaluated as a candidate radioligand was [^{11}C]MBMP. It has a high affinity (K_i = 0.29 nM) and specificity and shows higher binding potential than [^{11}C](*R*)-PK11195. However, this new radioligand has no important advantages over second-generation radioligands. More importantly, at 60 minutes after intravenous injection of [^{11}C]MBMP, more than 30% of radioactivity in the mouse brain was radiometabolite, a value remarkably higher than for other TSPO radioligands. Because this drawback would likely prevent the clinical use of [^{11}C]MBMP, no further evaluation has been performed [187]. To surmount this issue, ligands [^{18}F]FEBMP and [^{18}F]FPBMP were prepared as superior homologues. Both compounds had lower binding affinity than [^{11}C]MBMP (K_i = 3.9 nM) in rat brain homogenates, with the fluoroethoxy derivative [^{18}F]FEBMP (K_i = 6.6 nM) more active than the fluoropropoxy analogue [^{18}F]FPBMP (K_i = 16.7 nM). [^{18}F]FEBMP (log$D$ = 3.4) showed suitable lipophilicity for brain permeability, the same as [^{11}C]MBMP, and was selected for further evaluation [188]. *In vitro* autoradiography on post-mortem human brains suggested that binding sites of [^{18}F]FEBMP were little affected by SNP rs6971. However, the analysis showed rapid metabolism in plasma and radiometabolites in the brain (>20% of radioactivity at 60

minutes after injection). Therefore, [^{18}F]FEBMP did not yield a substantial improvement in metabolic stability relative to [^{11}C]MBMP [189]. With the aim to decrease lipophilicity and, putatively, to obtain more rapid brain kinetics and reduced nonspecific binding in target tissues, a series of benzoxazolones derivatives with a pyridine in place of the benzene ring was designed. The alkoxy linker between the label and the aromatic ring was also removed, placing fluorine-18 directly on the aromatic ring, a position that was expected to be more metabolically stable. 2-(5-(6-Fluoropyridin-3-yl)-2-oxobenzo[d]-oxazol-3(2*H*)-yl)-*N*-methyl-N-phenylacetamide (FPyBMP) exhibited adequate TSPO binding affinity (K_i = 13.4 nM) and moderate lipophilicity (log*D* = 1.92). [^{18}F]FPyBMP gave better brain kinetics than the previously developed benzoxazolones radioligands and provided a clear tumor image in a glioma-bearing rat model. At 30 minutes after injection, 93% of unchanged [^{11}C]FPyBMP was found in the ischemic rat brain, even if the compound was rapidly degraded in plasma [190]. To date, there are no data either on the effect on the binding by SNP rs6971 or on *in vivo* studies.

CONCLUSION

Increasing evidence shows that TSPO expression is altered in a variety of human diseases such as in cancer and in various neurological and psychiatric disorders. In particular, TSPO expression in the brain is considered a reliable marker of neuroinflammation and is correlated with pathophysiology in brain disorders such as Alzheimer's disease, Huntington's disease, multiple sclerosis, amyotrophic, lateral sclerosis, epilepsy, stroke and others. Therefore, TSPO quantification would allow the staging of the disease severity and, putatively, the evaluation of therapeutics and the measurement of neuroinflammation by PET imaging is becoming increasingly important.

After the development of the prototypical radioligand [^{11}C](*R*)-PK11195, various second-generation TSPO radioligands have been developed to overcome many of the limitations of this radioligand. Radioligands such as [^{18}F]FEPPA, [^{11}C]PBR06, [^{18}F]PBR111, [^{11}C]AC5216 and [^{18}F]PBR28 feature high affinity and selectively, better physicochemical properties and adequate pharmacokinetic characteristics. However, even if they are extensively studied as PET ligands for the quantification of TSPO in humans, the second-generation radioligands are sensitive to SNP rs6971 in the TSPO gene. This obstacle can be addressed by doing TSPO genotyping before imaging (to exclude low-affinity binders) and by including binding affinity as a statistical covariate.

To make TSPO imaging more useful in clinical settings, current efforts are focused on the development of TSPO specific radioligands that have the ideal characteristics of second-generation compounds but which are insensitive to the SNP rs6971. The first of these third-generation ligands is [^{11}C]ER176. It exhibits a high signal-to-noise ratio, proper pharmacokinetic properties, and, above all, is sufficiently insensitive to the SNP rs6971 to allow reliable TSPO measurement in low-affinity binders. Thus, evidence suggests that, to date, [^{11}C]ER176 is the best available TSPO radioligand for reliable quantification of neuroinflammation by PET imaging.

Overall, the availability of new radioligands renders TSPO imaging a quite remarkable method to define differences between patients and healthy humans. Nevertheless, an ideal TSPO radioligand does not yet exist; there is additional room for improvement.

FUNDING

SC and BC were supported by grants from the Italian Ministero dell'Istruzione, dell'Università e della Ricerca (MIUR), Progetti di Ricerca di Interesse Nazionale (PRIN 2017MT3993); FGS and VWP acknowledge support from the Intramural Research Program of the National Institutes of Health (National Institute of Mental Health, Project ZIA MH002793).

REFERENCES

1. Papadopoulos V; Baraldi M; Guilarte TR; Knudsen TB; Lacapère JJ; Lindemann P; Norenberg MD; Nutt D; Weizman A; Zhang MR; Gavish M Translocator protein (18kDa): New nomenclature for the peripheral-type benzodiazepine receptor based on its structure and molecular function. Trends Pharmacol. Sci, 2006, 27(8), 402–409. 10.1016/j.tips.2006.06.005 [PubMed: 16822554]
2. Li H; Papadopoulos V Peripheral-type benzodiazepine receptor function in cholesterol transport. Identification of a putative cholesterol recognition/interaction amino acid sequence and consensus pattern. Endocrinology, 1998, 139(12), 4991–4997. 10.1210/endo.139.12.6390 [PubMed: 9832438]
3. Lacapère JJ; Delavoie F; Li H; Péranzi G; Maccario J; Papadopoulos V; Vidic B Structural and functional study of reconstituted peripheral benzodiazepine receptor. Biochem. Biophys. Res. Commun, 2001, 284(2), 536–541. 10.1006/bbrc.2001.4975 [PubMed: 11394915]
4. Gatliff J; Campanella M TSPO: kaleidoscopic 18-kDa amid biochemical pharmacology, control and targeting of mitochondria. Biochem. J, 2016, 473(2), 107–121. 10.1042/BJ20150899 [PubMed: 26733718]
5. Jaremko L; Jaremko M; Giller K; Becker S; Zweckstetter M Structure of the mitochondrial translocator protein in complex with a diagnostic ligand. Science, 2014, 343(6177), 1363–1366. 10.1126/science.1248725 [PubMed: 24653034]
6. Jaremko M; Jaremko Ł; Jaipuria G; Becker S; Zweckstetter M Structure of the mammalian TSPO/PBR protein. Biochem. Soc. Trans, 2015, 43(4), 566–571. 10.1042/BST20150029 [PubMed: 26551694]
7. Jaremko Ł; Jaremko M; Giller K; Becker S; Zweckstetter M Conformational flexibility in the transmembrane protein TSPO. Chemistry, 2015, 21(46), 16555–16563. 10.1002/chem.201502314 [PubMed: 26394723]
8. Li F; Liu J; Zheng Y; Garavito RM; Ferguson-Miller S Protein structure. Crystal structures of translocator protein (TSPO) and mutant mimic of a human polymorphism. Science, 2015, 347(6221), 555–558. 10.1126/science.1260590 [PubMed: 25635101]
9. Guo Y; Kalathur RC; Liu Q; Kloss B; Bruni R; Ginter C; Kloppmann E; Rost B; Hendrickson WA Protein structure. Structure and activity of tryptophan-rich TSPO proteins. Science, 2015, 347(6221), 551–555. 10.1126/science.aaa1534 [PubMed: 25635100]
10. Papadopoulos V; Lecanu L Translocator protein (18 kDa) TSPO: An emerging therapeutic target in neurotrauma. Exp. Neurol, 2009, 219(1), 53–57. 10.1016/j.expneurol.2009.04.016 [PubMed: 19409385]
11. Costa B; Da Pozzo E; Martini C Translocator protein as a promising target for novel anxiolytics. Curr. Top. Med. Chem, 2012, 12(4), 270–285. 10.2174/156802612799078720 [PubMed: 22204481]
12. Da Pozzo E; Giacomelli C; Barresi E; Costa B; Taliani S; Passetti Fda.S.; Martini C Targeting the 18-kDa translocator protein: Recent perspectives for neuroprotection. Biochem. Soc. Trans, 2015, 43(4), 559–565. 10.1042/BST20150028 [PubMed: 26551693]
13. Veenman L; Gavish M The peripheral-type benzodiazepine receptor and the cardiovascular system. Implications for drug development. Pharmacol. Ther, 2006, 110(3), 503–524. 10.1016/j.pharmthera.2005.09.007 [PubMed: 16337685]

14. Maaser K; Grabowski P; Oezdem Y; Krahn A; Heine B; Stein H; Buhr H; Zeitz M; Scherübl H Up-regulation of the peripheral benzodiazepine receptor during human colorectal carcinogenesis and tumor spread. Clin. Cancer Res, 2005, 11(5), 1751–1756. 10.1158/1078-0432.CCR-04-1955 [PubMed: 15755996]

15. Hauet T; Yao ZX; Bose HS; Wall CT; Han Z; Li W; Hales DB; Miller WL; Culty M; Papadopoulos V Peripheral-type benzodiazepine receptor-mediated action of steroidogenic acute regulatory protein on cholesterol entry into leydig cell mitochondria. Mol. Endocrinol, 2005, 19(2), 540–554. 10.1210/me.2004-0307 [PubMed: 15498831]

16. Ritsner M; Modai I; Gibel A; Leschiner S; Silver H; Tsinovoy G; Weizman A; Gavish M Decreased platelet peripheral-type benzodiazepine receptors in persistently violent schizophrenia patients. J. Psychiatr. Res, 2003, 37(6), 549–556. 10.1016/S0022-3956(03)00055-4 [PubMed: 14563387]

17. Banati RB Visualising microglial activation *in vivo*. Glia, 2002, 40(2), 206–217. 10.1002/glia.10144 [PubMed: 12379908]

18. Trapani A; Palazzo C; de Candia M; Lasorsa FM; Trapani G Targeting of the translocator protein 18 kDa (TSPO): a valuable approach for nuclear and optical imaging of activated microglia. Bioconjug. Chem, 2013, 24(9), 1415–1428. 10.1021/bc300666f [PubMed: 23837837]

19. Nutma E; Ceyzériat K; Amor S; Tsartsalis S; Millet P; Owen DR; Papadopoulos V; Tournier BB Cellular sources of TSPO expression in healthy and diseased brain. Eur. J. Nucl. Med. Mol. Imaging, 2021, 49(1), 146–163. 10.1007/s00259-020-05166-2 [PubMed: 33433698]

20. Dupont AC; Largeau B; Santiago Ribeiro MJ; Guilloteau D; Tronel C; Arlicot N Translocator Protein-18 kDa (TSPO) Positron Emission Tomography (PET) Imaging and Its Clinical Impact in Neurodegenerative Diseases. Int. J. Mol. Sci, 2017, 18(4), 785–821. 10.3390/ijms18040785 [PubMed: 28387722]

21. Meyer JH; Cervenka S; Kim MJ; Kreisl WC; Henter ID; Innis RB Neuroinflammation in psychiatric disorders: PET imaging and promising new targets. Lancet Psychiatry, 2020, 7(12), 1064–1074. 10.1016/S2215-0366(20)30255-8 [PubMed: 33098761]

22. Notter T; Coughlin JM; Gschwind T; Weber-Stadlbauer U; Wang Y; Kassiou M; Vernon AC; Benke D; Pomper MG; Sawa A; Meyer UTranslational evaluation of translocator protein as a marker of neuroinflammation in schizophrenia. Mol. Psychiatry, 2018, 23(2), 323–334. 10.1038/mp.2016.248 [PubMed: 28093569]

23. Zhang XY; Wei W; Zhang YZ; Fu Q; Mi WD; Zhang LM; Li YF The 18 kDa Translocator Protein (TSPO) overexpression in hippocampal dentate gyrus elicits anxiolytic-like effects in a mouse model of post-traumatic stress disorder. Front. Pharmacol, 2018, 9, 1364–1374. 10.3389/fphar.2018.01364 [PubMed: 30532709]

24. Attwells S; Setiawan E; Wilson AA; Rusjan PM; Mizrahi R; Miler L; Xu C; Richter MA; Kahn A; Kish SJ; Houle S; Ravindran L; Meyer JH Inflammation in the neurocircuitry of obsessive-compulsive disorder. JAMA Psychiatry, 2017, 74(8), 833–840. 10.1001/jamapsychiatry.2017.1567 [PubMed: 28636705]

25. Favreau F; Rossard L; Zhang K; Desurmont T; Manguy E; Belliard A; Fabre S; Liu J; Han Z; Thuillier R; Papadopoulos V; Hauet T Expression and modulation of translocator protein and its partners by hypoxia reoxygenation or ischemia and reperfusion in porcine renal models. Am. J. Physiol. Renal Physiol, 2009, 297(1), F177–F190. 10.1152/ajprenal.90422.2008 [PubMed: 19386723]

26. Ran C; Albrecht DS; Bredella MA; Yang J; Yang J; Liang SH; Cypess AM; Loggia ML; Atassi N; Moore A PET imaging of human brown adipose tissue with the TSPO Tracer [^{11}C]PBR28. Mol. Imaging Biol, 2018, 20(2), 188–193. 10.1007/s11307-017-1129-z [PubMed: 28983743]

27. Herranz E; Giannì C; Louapre C; Treaba CA; Govindarajan ST; Ouellette R; Loggia ML; Sloane JA; Madigan N; Izquierdo-Garcia D; Ward N; Mangeat G; Granberg T; Klawiter EC; Catana C; Hooker JM; Taylor N; Ionete C; Kinkel RP; Mainero C Neuroinflammatory component of gray matter pathology in multiple sclerosis. Ann. Neurol, 2016, 80(5), 776–790. 10.1002/ana.24791 [PubMed: 27686563]

28. Zürcher NR; Loggia ML; Lawson R; Chonde DB; Izquierdo-Garcia D; Yasek JE; Akeju O; Catana C; Rosen BR; Cudkowicz ME; Hooker JM; Atassi N Increased *in vivo* glial activation in patients

with amyotrophic lateral sclerosis: assessed with [^{11}C]-PBR28. Neuroimage Clin., 2015, 7, 409–414. 10.1016/j.nicl.2015.01.009 [PubMed: 25685708]

29. Kreisl WC; Lyoo CH; Liow JS; Snow J; Page E; Jenko KJ; Morse CL; Zoghbi SS; Pike VW; Turner RS; Innis RB Distinct patterns of increased translocator protein in posterior cortical atrophy and amnestic Alzheimer's disease. Neurobiol. Aging, 2017, 51, 132–140. 10.1016/j.neurobiolaging.2016.12.006 [PubMed: 28068564]
30. Notter T; Coughlin JM; Sawa A; Meyer U Reconceptualization of translocator protein as a biomarker of neuroinflammation in psychiatry. Mol. Psychiatry, 2018, 23(1), 36–47. 10.1038/mp.2017.232 [PubMed: 29203847]
31. Wyatt SK; Manning HC; Bai M; Bailey SN; Gallant P; Ma G; McIntosh L; Bornhop DJ Molecular imaging of the translocator protein (TSPO) in a pre-clinical model of breast cancer. Mol. Imaging Biol, 2010, 12(3), 349–358. 10.1007/s11307-009-0270-8 [PubMed: 19949989]
32. Jiemy WF; Heeringa P; Kamps JAAM; van der Laken CJ; Slart RHJA; Brouwer E Positron emission tomography (PET) and single photon emission computed tomography (SPECT) imaging of macrophages in large vessel vasculitis: Current status and future prospects. Autoimmun. Rev, 2018, 17(7), 715–726. 10.1016/j.autrev.2018.02.006 [PubMed: 29729443]
33. Ametamey SM; Honer M; Schubiger PA Molecular imaging with PET. Chem. Rev, 2008, 108(5), 1501–1516. 10.1021/cr0782426 [PubMed: 18426240]
34. Kreisl WC; Kim MJ; Coughlin JM; Henter ID; Owen DR; Innis RB PET imaging of neuroinflammation in neurological disorders. Lancet Neurol., 2020, 19(11), 940–950. 10.1016/S1474-4422(20)30346-X [PubMed: 33098803]
35. Narayanaswami V; Dahl K; Bernard-Gauthier V; Josephson L; Cumming P; Vasdev N Emerging PET radiotracers and targets for imaging of neuroinflammation in neurodegenerative diseases: Outlook beyond TSPO. Mol. Imaging, 2018, 17, 1536012118792317. 10.1177/1536012118792317 [PubMed: 30203712]
36. Lagarde J; Sarazin M; Bottlaender M *In vivo* PET imaging of neuroinflammation in Alzheimer's disease. J. Neural Trans , 2018, 125(5), 847–867.
37. Werry EL; Bright FM; Piguet O; Ittner LM; Halliday GM; Hodges JR; Kiernan MC; Loy CT; Kril JJ; Kassiou M Recent developments in TSPO PET imaging as a biomarker of neuroinflammation in neurodegenerative disorders. Int. J. Mol. Sci, 2019, 20(13), 3161–3181. 10.3390/ijms20133161 [PubMed: 31261683]
38. Patel S; Gibson R *In vivo* site-directed radiotracers: A mini-review. Nucl. Med. Biol, 2008, 35(8), 805–815. 10.1016/j.nucmedbio.2008.10.002 [PubMed: 19026942]
39. Laruelle M; Slifstein M; Huang Y Relationships between radiotracer properties and image quality in molecular imaging of the brain with positron emission tomography. Mol. Imaging Biol, 2003, 5(6), 363–375. 10.1016/j.mibio.2003.09.009 [PubMed: 14667491]
40. Waterhouse RN Determination of lipophilicity and its use as a predictor of blood-brain barrier penetration of molecular imaging agents. Mol. Imaging Biol, 2003, 5(6), 376–389. 10.1016/j.mibio.2003.09.014 [PubMed: 14667492]
41. Pike VW Considerations in the development of reversibly binding PET radioligands for brain imaging. Curr. Med. Chem, 2016, 23(18), 1818–1869. 10.2174/0929867323666160418114826 [PubMed: 27087244]
42. Hall MD; Pike VW Avoiding barriers to PET radioligand development: Cellular assays of brain efflux transporters. J. Nuclear Med, 2011, 52(3), 338–340.
43. Pike VW PET radiotracers: crossing the blood-brain barrier and surviving metabolism. Trends Pharmacol. Sci, 2009, 30(8), 431–440. 10.1016/j.tips.2009.05.005 [PubMed: 19616318]
44. Kreisl WC; Fujita M; Fujimura Y; Kimura N; Jenko KJ; Kannan P; Hong J; Morse CL; Zoghbi SS; Gladding RL; Jacobson S; Oh U; Pike VW; Innis RB Comparison of [^{11}C]-(R)-PK 11195 and [^{11}C]PBR28, two radioligands for translocator protein (18 kDa) in human and monkey: Implications for positron emission tomographic imaging of this inflammation biomarker. Neuroimage, 2010, 49(4), 2924–2932. 10.1016/j.neuroimage.2009.11.056 [PubMed: 19948230]
45. Zhang L; Villalobos A; Beck EM; Bocan T; Chappie TA; Chen L; Grimwood S; Heck SD; Helal CJ; Hou X; Humphrey JM; Lu J; Skaddan MB; Mc-Carthy TJ; Verhoest PR; Wager TT; Zasadny K Design and selection parameters to accelerate the discovery of novel central nervous system

positron emission tomography (PET) ligands and their application in the development of a novel phosphodiesterase 2A PET ligand. J. Med. Chem, 2013, 56(11), 4568–4579. 10.1021/jm400312y [PubMed: 23651455]

46. Cho ZH; Chan JK; Ericksson L; Singh M; Graham S; MacDonald NS; Yano Y Positron ranges obtained from biomedically important positron-emitting radionuclides. J. Nuclear Med, 1975, 16(12), 1174–1176.
47. Carter LM; Kesner AL; Pratt EC; Sanders VA; Massicano AVF; Cutler CS; Lapi SE; Lewis JS The impact of positron range on PET resolution, evaluated with phantoms and PHITS Monte Carlo simulations for conventional and non-conventional radionuclides. Mol. Imaging Biol, 2020, 22(1), 73–84. 10.1007/s11307-019-01337-2 [PubMed: 31001765]
48. Zanotti-Fregonara P; Lammertsma AA; Innis RB ^{11}C dosimetry scans should be abandoned. J. Nuclear Med, 2021, 62(2), 158–159.
49. Patani GA; LaVoie EJ Bioisosterism: A rational approach in drug design. Chem. Rev, 1996, 96(8), 3147–3176. 10.1021/cr950066q [PubMed: 11848856]
50. Meanwell NA Synopsis of some recent tactical application of bioisosteres in drug design. J. Med. Chem, 2011, 54(8), 2529–2591. 10.1021/jm1013693 [PubMed: 21413808]
51. Meanwell NA Fluorine and fluorinated motifs in the design and application of bioisosteres for drug design. J. Med. Chem, 2018, 61(14), 5822–5880. 10.1021/acs.jmedchem.7b01788 [PubMed: 29400967]
52. Fujita M; Imaizumi M; Zoghbi SS; Fujimura Y; Farris AG; Suhara T; Hong J; Pike VW; Innis RB Kinetic analysis in healthy humans of a novel positron emission tomography radioligand to image the peripheral benzodiazepine receptor, a potential biomarker for inflammation. Neuroimage, 2008, 40(1), 43–52. 10.1016/j.neuroimage.2007.11.011 [PubMed: 18093844]
53. Owen DR; Howell OW; Tang SP; Wells LA; Bennacef I; Bergstrom M; Gunn RN; Rabiner EA; Wilkins MR; Reynolds R; Matthews PM; Parker CA Two binding sites for [^{3}H]PBR28 in human brain: Implications for TSPO PET imaging of neuroinflammation. J. Cereb. Blood Flow Metab, 2010, 30(9), 1608–1618. 10.1038/jcbfm.2010.63 [PubMed: 20424634]
54. Owen DR; Yeo AJ; Gunn RN; Song K; Wadsworth G; Lewis A; Rhodes C; Pulford DJ; Bennacef I; Parker CA; StJean PL; Cardon LR; Mooser VE; Matthews PM; Rabiner EA; Rubio JP An 18-kDa translocator protein (TSPO) polymorphism explains differences in binding affinity of the PET radioligand PBR28. J. Cereb. Blood Flow Metab, 2012, 32(1), 1–5. 10.1038/jcbfm.2011.147 [PubMed: 22008728]
55. Owen DR; Guo Q; Rabiner EA; Gunn RN The impact of the rs6971 polymorphism in TSPO for quantification and study design. Clin. Transl. Imaging, 2015, 3(6), 417–422. 10.1007/s40336-015-0141-z
56. Taliani S; Pugliesi I; Da Settimo F Structural requirements to obtain highly potent and selective 18 kDa Translocator Protein (TSPO) Ligands. Curr. Top. Med. Chem, 2011, 11(7), 860–886. 10.2174/156802611795165142 [PubMed: 21291396]
57. Junck L; Olson JM; Ciliax BJ; Koeppe RA; Watkins GL; Jewett DM; McKeever PE; Wieland DM; Kilbourn MR; Starosta-Rubinstein S PET imaging of human gliomas with ligands for the peripheral benzodiazepine binding site. Ann. Neurol, 1989, 26(6), 752–758. 10.1002/ana.410260611 [PubMed: 2557794]
58. Farges R; Joseph-Liauzun E; Shire D; Caput D; Le Fur G; Ferrara P Site-directed mutagenesis of the peripheral benzodiazepine receptor: Identification of amino acids implicated in the binding site of Ro5-4864. Mol. Pharmacol, 1994, 46(6), 1160–1167. [PubMed: 7808437]
59. Van Dort ME; Ciliax BJ; Gildersleeve DL; Sherman PS; Rosenspire KC; Young AB; Junck L; Wieland DM Radioiodinated benzodiazepines: Agents for mapping glial tumors. J. Med. Chem, 1988, 31(11), 2081–2086. 10.1021/jm00119a005 [PubMed: 2846836]
60. Camsonne R; Crouzel C; Comar D; Mazière M; Prenant C; Sastre J; Moulin M; Syrota A Synthesis of N-(11C) methyl, N-(methyl-1 propyl), (chloro-2 phenyl)-1 isoquinoleine carboxamide-3 (PK 11195): A new ligand for peripheral benzodiazepine receptors. 1984, 21(10), 985–991.
61. Shah F; Hume SP; Pike VW; Ashworth S; McDermott J Synthesis of the enantiomers of [N-methyl-^{11}C]PK11195 and comparison of their behaviours as radioligands for PK binding sites in rats. Nucl. Med. Biol, 1994, 21(4), 573–581. 10.1016/0969-8051(94)90022-1 [PubMed: 9234314]

62. Tondo G; Boccalini C; Caminiti SP; Presotto L; Filippi M; Magnani G; Frisoni GB; Iannaccone S; Perani D Brain metabolism and microglia activation in mild cognitive impairment: A combined [^{18}F]FDG and [^{11}C]-(R)-PK11195 PET study. J. Alzheimers Dis, 2021, 80(1), 433–445. 10.3233/JAD-201351 [PubMed: 33579848]

63. Tondo G; Iaccarino L; Cerami C; Vanoli GE; Presotto L; Masiello V; Coliva A; Salvi F; Bartolomei I; Mosca L; Lunetta C; Perani D ^{11}C-PK11195 PET-based molecular study of microglia activation in SOD1 amyotrophic lateral sclerosis. Ann. Clin. Transl. Neurol, 2020, 7(9), 1513–1523. 10.1002/acn3.51112 [PubMed: 32762033]

64. van der Doef TF; de Witte LD; Sutterland AL; Jobse E; Yaqub M; Boellaard R; de Haan L; Eriksson J; Lammertsma AA; Kahn RS; van Berckel BN *In vivo* (R)-[^{11}C]PK11195 PET imaging of 18kDa translocator protein in recent onset psychosis. NPJ Schizophr., 2016, 2(1), 16031–16035. 10.1038/npjschz.2016.31 [PubMed: 27602389]

65. Seo S; Jung YH; Lee D; Lee WJ; Jang JH; Lee JY; Choi SH; Moon JY; Lee JS; Cheon GJ; Kang H Abnormal neuroinflammation in fibromyalgia and CRPS using [^{11}C]-(R)-PK11195 PET. PLoS One, 2021, 16(2), e0246152.10.1371/journal.pone.0246152 [PubMed: 33556139]

66. Iaccarino L; Moresco RM; Presotto L; Bugiani O;Iannaccone S; Giaccone G; Tagliavini F; Perani D An *in vivo* ^{11}C-(R)-PK11195 PET and *in vitro* pathology study of microglia activation in creutzfeldt-jakob disease. Mol. Neurobiol, 2018, 55(4), 2856–2868. 10.1007/s12035-017-0522-6 [PubMed: 28455699]

67. Chauveau F; Boutin H; Van Camp N; Dollé F; Tavitian B Nuclear imaging of neuroinflammation: A comprehensive review of [^{11}C]PK11195 challengers. Eur. J. Nucl. Med. Mol. Imaging, 2008, 35(12), 2304–2319. 10.1007/s00259-008-0908-9 [PubMed: 18828015]

68. Schuitemaker A; van Berckel BN; Kropholler MA; Veltman DJ; Scheltens P; Jonker C; Lammertsma AA; Boellaard R SPM analysis of parametric (R)-[^{11}C]PK11195 binding images: plasma input versus reference tissue parametric methods. Neuroimage, 2007, 35(4), 1473–1479. 10.1016/j.neuroimage.2007.02.013 [PubMed: 17363280]

69. Parente A; Feltes PK; Vállez García D; Sijbesma JW; Moriguchi Jeckel CM; Dierckx RA; de Vries EF; Doorduin J Pharmacokinetic analysis of 11C-PBR28 in the rat model of herpes encephalitis: Comparison with (R)-11C-PK11195. J. Nuclear Med, 2016, 57(5), 785–791.

70. Pascali C; Luthra SK; Pike VW; Price GW; Ahier RG; Hume SP; Myers R; Manjil L; Cremer JE The radiosynthesis of [^{18}F]PK 14105 as an alternative radioligand for peripheral type benzodiazepine binding sites. Int. J. Rad. Appl. Instrum. [A], 1990, 41(5), 477–482. 10.1016/0883-2889(90)90008-5

71. Price GW; Ahier RG; Hume SP; Myers R; Manjil L; Cremer JE; Luthra SK; Pascali C; Pike V; Frackowiak RS *In vivo* binding to peripheral benzodiazepine binding sites in lesioned rat brain: Comparison between [^{3}H]PK11195 and [^{18}F]PK14105 as markers for neuronal damage. J. Neurochem, 1990, 55(1), 175–185. 10.1111/j.1471-4159.1990.tb08836.x [PubMed: 2355218]

72. Matarrese M; Moresco RM; Cappelli A; Anzini M; Vomero S; Simonelli P; Verza E; Magni F; Sudati F; Soloviev D; Todde S; Carpinelli A; Kienle MG; Fazio F Labeling and evaluation of N-[^{11}C]methylated quinoline-2-carboxamides as potential radioligands for visualization of peripheral benzodiazepine receptors. J. Med. Chem, 2001, 44(4), 579–585. 10.1021/jm001004h [PubMed: 11170647]

73. Belloli S; Moresco RM; Matarrese M; Biella G; Sanvito F; Simonelli P; Turolla E; Olivieri S; Cappelli A; Vomero S; Galli-Kienle M; Fazio F Evaluation of three quinoline-carboxamide derivatives as potential radioligands for the *in vivo* pet imaging of neurodegeneration. Neurochem. Int, 2004, 44(6), 433–440. 10.1016/j.neuint.2003.08.006 [PubMed: 14687608]

74. Cappelli A; Matarrese M; Moresco RM; Valenti S;Anzini M; Vomero S; Turolla EA; Belloli S; Simonelli P; Filannino MA; Lecchi M; Fazio F Synthesis, labeling, and biological evaluation of halogenated 2-quinolinecarboxamides as potential radioligands for the visualization of peripheral benzodiazepine receptors. Bioorg. Med. Chem, 2006, 14(12), 4055–4066. 10.1016/j.bmc.2006.02.004 [PubMed: 16495062]

75. Di Grigoli G; Monterisi C; Belloli S; Masiello V; Politi LS; Valenti S; Paolino M; Anzini M; Matarrese M; Cappelli A; Moresco RM Radiosynthesis and preliminary biological evaluation of [^{18}F]VC701, a Radioligand for translocator protein. Mol. Imaging, 2015, 14(6), 14–22. 10.2310/7290.2015.00007

76. Castellano S; Taliani S; Milite C; Pugliesi I; Da Pozzo E; Rizzetto E; Bendinelli S; Costa B; Cosconati S; Greco G; Novellino E; Sbardella G; Stefancich G; Martini C; Da Settimo F Synthesis and biological evaluation of 4-phenylquinazoline-2-carboxamides designed as a novel class of potent ligands of the translocator protein. J. Med. Chem, 2012, 55(9), 4506–4510. 10.1021/jm201703k [PubMed: 22489952]
77. Castellano S; Taliani S; Viviano M; Milite C; Da Pozzo E; Costa B; Barresi E; Bruno A; Cosconati S; Marinelli L; Greco G; Novellino E; Sbardella G; Da Settimo F; Martini C Structure-activity relationship refinement and further assessment of 4-phenylquinazoline-2-carboxamide translocator protein ligands as antiproliferative agents in human glioblastoma tumors. J. Med. Chem, 2014, 57(6), 2413–2428. 10.1021/jm401721h [PubMed: 24580635]
78. Zanotti-Fregonara P; Zhang Y; Jenko KJ; Gladding RL; Zoghbi SS; Fujita M; Sbardella G; Castellano S; Taliani S; Martini C; Innis RB; Da Settimo F; Pike VW Synthesis and evaluation of translocator 18 kDa protein (TSPO) positron emission tomography (PET) radioligands with low binding sensitivity to human single nucleotide polymorphism rs6971. ACS Chem. Neurosci, 2014, 5(10), 963–971. 10.1021/cn500138n [PubMed: 25123416]
79. Ikawa M; Lohith TG; Shrestha S; Telu S; Zoghbi SS; Castellano S; Taliani S; Da Settimo F; Fujita M; Pike VW; Innis RB 11c-er176, a radioligand for 18-kda translocator protein, has adequate sensitivity to robustly image all three affinity genotypes in human brain. J. Nuclear Med, 2017, 58(2), 320–325.
80. Zanotti-Fregonara P; Pascual B; Veronese M; Yu M; Beers D; Appel SH; Masdeu JC Head-to-head comparison of ^{11}C-PBR28 and ^{11}C-ER176 for quantification of the translocator protein in the human brain. Eur. J. Nucl. Med. Mol. Imaging, 2019, 46(9), 1822–1829. 10.1007/s00259-019-04349-w [PubMed: 31152207]
81. Fujita M; Kobayashi M; Ikawa M; Gunn RN; Rabiner EA; Owen DR; Zoghbi SS; Haskali MB; Telu S; Pike VW; Innis RB Comparison of four ^{11}C-labeled PET ligands to quantify translocator protein 18 kDa (TSPO) in human brain: (R)-PK11195, PBR28, DPA-713, and ER176-based on recent publications that measured specific-to-non-displaceable ratios. EJNMMI Res., 2017, 7(1), 84–88. 10.1186/s13550-017-0334-8 [PubMed: 29038960]
82. Downer OM; Marcus REG; Zürcher NR; Hooker JM Tracing the history of the human translocator protein to recent neurodegenerative and psychiatric imaging. ACS Chem. Neurosci, 2020, 11(15), 2192–2200. 10.1021/acschemneuro.0c00362 [PubMed: 32662626]
83. Hong J; Telu S; Zhang Y; Miller WH; Shetty HU; Morse CL; Pike VW Translation of ^{11}C-labeled tracer synthesis to a CGMP environment as exemplified by [^{11}C]ER176 for PET imaging of human TSPO. Nat. Protoc, 2021, 16(9), 4419–4445. 10.1038/s41596-021-00584-4 [PubMed: 34363068]
84. Siméon FG; Lee JH; Morse CL; Stukes I; Zoghbi SS; Manly LS; Liow JS; Gladding RL; Dick RM; Yan X; Taliani S; Costa B; Martini C; Da Settimo F; Castellano S; Innis RB; Pike VW Synthesis and screening in mice of fluorine-containing PET radioligands for TSPO: discovery of a promising ^{18}F-labeled ligand. J. Med. Chem, 2021, 64(22), 16731–16745. 10.1021/acs.jmedchem.1c01562 [PubMed: 34756026]
85. Okuyama S; Chaki S; Yoshikawa R; Ogawa S; Suzuki Y; Okubo T; Nakazato A; Nagamine M; Tomisawa K Neuropharmacological profile of peripheral benzodiazepine receptor agonists, DAA1097 and DAA1106. Life Sci., 1999, 64(16), 1455–1464. 10.1016/S0024-3205(99)00079-X [PubMed: 10321725]
86. Zhang MR; Kida T; Noguchi J; Furutsuka K; Maeda J; Suhara T; Suzuki K [^{11}C]DAA1106: Radiosynthesis and *in vivo* binding to peripheral benzodiazepine receptors in mouse brain. Nucl. Med. Biol, 2003, 30(5), 513–519. 10.1016/S0969-8051(03)00016-7 [PubMed: 12831989]
87. Venneti S; Lopresti BJ; Wang G; Slagel SL; Mason NS; Mathis CA; Fischer ML; Larsen NJ; Mortimer AD; Hastings TG; Smith AD; Zigmond MJ; Suhara T; Higuchi M; Wiley CA A comparison of the high-affinity peripheral benzodiazepine receptor ligands DAA1106 and (R)-PK11195 in rat models of neuroinflammation: implications for PET imaging of microglial activation. J. Neurochem, 2007, 102(6), 2118–2131. 10.1111/j.1471-4159.2007.04690.x [PubMed: 17555551]

88. Venneti S; Wang G; Nguyen J; Wiley CA The positron emission tomography ligand DAA1106 binds with high affinity to activated microglia in human neurological disorders. J. Neuropathol. Exp. Neurol, 2008, 67(10), 1001–1010. 10.1097/NEN.0b013e318188b204 [PubMed: 18800007]

89. Yasuno F; Ota M; Kosaka J; Ito H; Higuchi M; Doronbekov TK; Nozaki S; Fujimura Y; Koeda M; Asada T; Suhara T Increased binding of peripheral benzodiazepine receptor in Alzheimer's disease measured by positron emission tomography with [^{11}C]DAA1106. Biol. Psychiatry, 2008, 64(10), 835–841. 10.1016/j.biopsych.2008.04.021 [PubMed: 18514164]

90. Takano A; Arakawa R; Ito H; Tateno A; Takahashi H; Matsumoto R; Okubo Y; Suhara T Peripheral benzodiazepine receptors in patients with chronic schizophrenia: a PET study with [^{11}C]DAA1106. Int. J. Neuropsychopharmacol, 2010, 13(7), 943–950. 10.1017/S1461145710000313 [PubMed: 20350336]

91. Brody AL; Hubert R; Enoki R; Garcia LY; Mamoun MS; Okita K; London ED; Nurmi EL; Seaman LC; Mandelkern MA Effect of cigarette smoking on a marker for neuroinflammation: A [^{11}C]DAA1106 Positron Emission Tomography study. Neuropsychopharmacology, 2017, 42(8), 1630–1639. [PubMed: 28262740]

92. Brody AL; Gehlbach D; Garcia LY; Enoki R; Hoh C; Vera D; Kotta KK; London ED; Okita K; Nurmi EL; Seaman LC; Mandelkern MA Effect of overnight smoking abstinence on a marker for microglial activation: A [^{11}C]DAA1106 positron emission tomography study. Psychopharmacology (Berl.), 2018, 235(12), 3525–3534. 10.1007/s00213-018-5077-3 [PubMed: 30343364]

93. Zhang MR; Maeda J; Furutsuka K; Yoshida Y; Ogawa M; Suhara T; Suzuki K [^{18}F]FMDAA1106 and [^{18}F]FEDAA1106: two positron-emitter labeled ligands for peripheral benzodiazepine receptor (PBR). Bioorg. Med. Chem. Lett, 2003, 13(2), 201–204. 10.1016/S0960-894X(02)00886-7 [PubMed: 12482423]

94. Zhang MR; Maeda J; Ogawa M; Noguchi J; Ito T; Yoshida Y; Okauchi T; Obayashi S; Suhara T; Suzuki K Development of a new radioligand, N-(5-fluoro-2-phenoxyphenyl)-N-(2-[^{18}F]fluoroethyl-5-methoxybenzyl)acetamide, for pet imaging of peripheral benzodiazepine receptor in primate brain. J. Med. Chem, 2004, 47(9), 2228–2235. 10.1021/jm0304919 [PubMed: 15084121]

95. Fujimura Y; Ikoma Y; Yasuno F; Suhara T; Ota M; Matsumoto R; Nozaki S; Takano A; Kosaka J; Zhang MR; Nakao R; Suzuki K; Kato N; Ito H Quantitative analyses of ^{18}F-FEDAA1106 binding to peripheral benzodiazepine receptors in living human brain. Journal of nuclear medicine , 2006, 47(1), 43–50. [PubMed: 16391186]

96. Varrone A; Mattsson P; Forsberg A; Takano A; Nag S; Gulyás B; Borg J; Boellaard R; Al-Tawil N; Eriksdotter M; Zimmermann T; Schultze-Mosgau M; Thiele A; Hoffmann A; Lammertsma AA; Halldin C *In vivo* imaging of the 18-kDa translocator protein (TSPO) with [^{18}F]FEDAA1106 and PET does not show increased binding in Alzheimer's disease patients. Eur. J. Nucl. Med. Mol. Imaging, 2013, 40(6), 921–931. 10.1007/s00259-013-2359-1 [PubMed: 23436070]

97. Briard E; Zoghbi SS; Siméon FG; Imaizumi M; Gourley JP; Shetty HU; Lu S; Fujita M; Innis RB; Pike VW Single-step high-yield radiosynthesis and evaluation of a sensitive ^{18}F-labeled ligand for imaging brain peripheral benzodiazepine receptors with PET. J. Med. Chem, 2009, 52(3), 688–699. 10.1021/jm8011855 [PubMed: 19119848]

98. Fujimura Y; Kimura Y; Siméon FG; Dickstein LP; Pike VW; Innis RB; Fujita M Biodistribution and radiation dosimetry in humans of a new PET ligand, ^{18}F-PBR06, to image translocator protein (18 kDa). J. Nuclear Med, 2010, 51(1), 145–149.

99. Imaizumi M; Briard E; Zoghbi SS; Gourley JP; Hong J; Musachio JL; Gladding R; Pike VW; Innis RB; Fujita M Kinetic evaluation in nonhuman primates of two new PET ligands for peripheral benzodiazepine receptors in brain. Synapse, 2007, 61(8), 595–605. 10.1002/syn.20394 [PubMed: 17455247]

100. Simmons DA; James ML; Belichenko NP; Semaan S; Condon C; Kuan J; Shuhendler AJ; Miao Z; Chin FT; Longo FM TSPO-PET imaging using [^{18}F]PBR06 is a potential translatable biomarker for treatment response in Huntington's disease: preclinical evidence with the p75NTR ligand LM11A-31. Hum. Mol. Genet, 2018, 27(16), 2893–2912. 10.1093/hmg/ddy202 [PubMed: 29860333]

101. Lartey FM; Ahn GO; Ali R; Rosenblum S; Miao Z; Arksey N; Shen B; Colomer MV; Rafat M; Liu H; Alejandre-Alcazar MA; Chen JW; Palmer T; Chin FT; Guzman R; Loo BW Jr; Graves E The relationship between serial [^{18} F]PBR06 PET imaging of microglial activation and motor function following stroke in mice. Mol. Imaging Biol, 2014, 16(6), 821–829. 10.1007/s11307-014-0745-0 [PubMed: 24865401]

102. Briard E; Zoghbi SS; Imaizumi M; Gourley JP; Shetty HU; Hong J; Cropley V; Fujita M; Innis RB; Pike VW Synthesis and evaluation in monkey of two sensitive ^{11}C-labeled aryloxyanilide ligands for imaging brain peripheral benzodiazepine receptors *in vivo*. J. Med. Chem, 2008, 51(1), 17–30. 10.1021/jm0707370 [PubMed: 18067245]

103. Imaizumi M; Briard E; Zoghbi SS; Gourley JP; Hong J; Fujimura Y; Pike VW; Innis RB; Fujita M Brain and whole-body imaging in nonhuman primates of [^{11}C]PBR28, a promising PET radioligand for peripheral benzodiazepine receptors. Neuroimage, 2008, 39(3), 1289–1298. 10.1016/j.neuroimage.2007.09.063 [PubMed: 18024084]

104. Kreisl WC; Lyoo CH; Liow JS; Wei M; Snow J; Page E; Jenko KJ; Morse CL; Zoghbi SS; Pike VW; Turner RS; Innis RB ^{11}C-PBR28 binding to translocator protein increases with progression of Alzheimer's disease. Neurobiol. Aging, 2016, 44, 53–61. 10.1016/j.neurobiolaging.2016.04.011 [PubMed: 27318133]

105. Zou J; Tao S; Johnson A; Tomljanovic Z; Polly K; Klein J; Razlighi QR; Brickman AM; Lee S; Stern Y; Kreisl WC Microglial activation, but not tau pathology, is independently associated with amyloid positivity and memory impairment. Neurobiol. Aging, 2020, 85, 11–21. 10.1016/j.neurobiolaging.2019.09.019 [PubMed: 31698286]

106. Barletta VT; Herranz E; Treaba CA; Ouellette R; Mehndiratta A; Loggia ML; Klawiter EC; Ionete C; Jacob SA; Mainero C Evidence of diffuse cerebellar neuroinflammation in multiple sclerosis by ^{11}C-PBR28 MR-PET. Mult. Scler, 2020, 26(6), 668–678. 10.1177/1352458519843048 [PubMed: 30973800]

107. Zürcher NR; Loggia ML; Mullett JE; Tseng C;Bhanot A; Richey L; Hightower BG; Wu C; Parmar AJ; Butterfield RI; Dubois JM; Chonde DB; Izquierdo-Garcia D; Wey HY; Catana C; Hadjikhani N; McDougle CJ; Hooker JM [^{11}C]PBR28 MR-PET imaging reveals lower regional brain expression of translocator protein (TSPO) in young adult males with autism spectrum disorder. Mol. Psychiatry, 2021, 26(5), 1659–1669. 10.1038/s41380-020-0682-z [PubMed: 32076115]

108. Lois C; González I; Izquierdo-García D; Zürcher NR; Wilkens P; Loggia ML; Hooker JM; Rosas HD Neuroinflammation in Huntington's Disease: New Insights with ^{11}C-PBR28 PET/MRI. ACS Chem. Neurosci, 2018, 9(11), 2563–2571. 10.1021/acschemneuro.8b00072 [PubMed: 29719953]

109. Forsberg A; Lampa J; Estelius J; Cervenka S; Farde L; Halldin C; Lekander M; Olgart Höglund C; Kosek E Disease activity in rheumatoid arthritis is inversely related to cerebral TSPO binding assessed by [^{11}C]PBR28 positron emission tomography. J. Neuroimmunol, 2019, 334, 577000–577008. 10.1016/j.jneuroim.2019.577000 [PubMed: 31260948]

110. Hillmer AT; Matuskey D; Huang Y; Nabulsi N; Ropchan J; Carson RE; O'Malley SS; Cosgrove KP Tobacco smoking in people is not associated with altered 18-kDa translocator protein levels: A PET Study. J. Nuclear Med, 2020, 61(8), 1200–1204.

111. Owen DR; Gunn RN; Rabiner EA; Bennacef I; Fujita M; Kreisl WC; Innis RB; Pike VW; Reynolds R; Matthews PM; Parker CA Mixed-affinity binding in humans with 18-kDa translocator protein ligands. J. Nuclear Med, 2011, 52(1), 24–32.

112. Moon BS; Kim BS; Park C; Jung JH; Lee YW; Lee HY; Chi DY; Lee BC; Kim SE [^{11}F]Fluoromethyl-PBR28 as a potential radiotracer for TSPO: preclinical comparison with [^{11}C]PBR28 in a rat model of neuroinflammation. Bioconjug. Chem, 2014, 25(2), 442–450. 10.1021/bc400556h [PubMed: 24400917]

113. Kim GR; Paeng JC; Jung JH; Moon BS; Lopalco A; Denora N; Lee BC; Kim SE Assessment of TSPO in a rat experimental autoimmune myocarditis model: A comparison study between [^{11}F]Fluoromethyl-PBR28 and[^{11}F]CB251. Int. J. Mol. Sci, 2018, 19(1), 276–285. 10.3390/ijms19010276 [PubMed: 29342117]

114. Wilson AA; Garcia A; Parkes J; McCormick P; Stephenson KA; Houle S; Vasdev N Radiosynthesis and initial evaluation of [^{18}F]-FEPPA for PET imaging of

peripheral benzodiazepine receptors. Nucl. Med. Biol, 2008, 35(3), 305–314. 10.1016/j.nucmedbio.2007.12.009 [PubMed: 18355686]

115. Rusjan PM; Wilson AA; Bloomfield PM; Vitcu I; Meyer JH; Houle S; Mizrahi R Quantitation of translocator protein binding in human brain with the novel radioligand [^{18}F]-FEPPA and positron emission tomography. J. Cereb. Blood Flow Metab, 2011, 31(8), 1807–1816. 10.1038/jcbfm.2011.55 [PubMed: 21522163]
116. Mizrahi R; Rusjan PM; Kennedy J; Pollock B; Mulsant B; Suridjan I; De Luca V; Wilson AA; Houle S Translocator protein (18 kDa) polymorphism (rs6971) explains in-vivo brain binding affinity of the PET radioligand [^{11}F]-FEPPA. J. Cereb. Blood Flow Metab, 2012, 32(6), 968–972. 10.1038/jcbfm.2012.46 [PubMed: 22472607]
117. Ghadery C; Koshimori Y; Christopher L; Kim J; Rusjan P; Lang AE; Houle S; Strafella AP The interaction between neuroinflammation and β-Amyloid in cognitive decline in Parkinson's Disease. Mol. Neurobiol, 2020, 57(1), 492–501. 10.1007/s12035-019-01714-6 [PubMed: 31385228]
118. Suridjan I; Pollock BG; Verhoeff NP; Voineskos AN; Chow T; Rusjan PM; Lobaugh NJ; Houle S; Mulsant BH; Mizrahi R *In-vivo* imaging of grey and white matter neuroinflammation in Alzheimer's disease: A positron emission tomography study with a novel radioligand, [^{18}F]-FEPPA. Mol. Psychiatry, 2015, 20(12), 1579–1587. 10.1038/mp.2015. [PubMed: 25707397]
119. Hafizi S; Da Silva T; Meyer JH; Kiang M; Houle S; Remington G; Prce I; Wilson AA; Rusjan PM; Sailasuta N; Mizrahi R Interaction between TSPO-a neuroimmune marker-and redox status in clinical high risk for psychosis: A PET-MRS study. Neuropsychopharmacology, 2018, 43(8), 1700–1705. [PubMed: 29748630]
120. Damont A; Boisgard R; Kuhnast B; Lemee F; Raggiri G; Scarf AM; Da Pozzo E; Selleri S; Martini C; Tavitian B; Kassiou M; Dollé F Synthesis of 6-[^{1} F]fluoro-PBR28, a novel radiotracer for imaging the TSPO 18 kDa with PET. Bioorg. Med. Chem. Lett, 2011, 21(16), 4819–4822. 10.1016/j.bmcl.2011.06.048 [PubMed: 21741237]
121. Boutin H; Chauveau F; Thominiaux C; Kuhnast B; Grégoire MC; Jan S; Trebossen R; Dollé F; Tavitian B; Mattner F; Katsifis A *In vivo* imaging of brain lesions with [^{11}C]CLINME, a new PET radioligand of peripheral benzodiazepine receptors. Glia, 2007, 55(14), 1459–1468. 10.1002/glia.20562 [PubMed: 17680643]
122. Mattner F; Bandin DL; Staykova M; Berghofer P; Gregoire MC; Ballantyne P; Quinlivan M; Fordham S; Pham T; Willenborg DO; Katsifis A Evaluation of [^{123}I]-CLINDE as a potent SPECT radiotracer to assess the degree of astroglia activation in cuprizone-induced neuroinflammation. Eur. J. Nucl. Med. Mol. Imaging, 2011, 38(8), 1516–1528. 10.1007/s00259-011-1784-2 [PubMed: 21484375]
123. Bourdier T; Henderson D; Fookes CJ; Lam P; Mattner F; Fulham M; Katsifis A Synthesis of [^{11}C]PBR170,a novel imidazopyridine, for imaging the translocator protein with PET. Appl. Radiat. Isotopes, 2014, 90, 46–52.
124. Sekimata K; Hatano K; Ogawa M; Abe J; Magata Y; Biggio G; Serra M; Laquintana V; Denora N; Latrofa A; Trapani G; Liso G; Ito K Radiosynthesis and *in vivo* evaluation of N-[^{11}C]methylated imidazopyridineacetamides as PET tracers for peripheral benzodiazepine receptors. Nucl. Med. Biol, 2008, 35(3), 327–334. 10.1016/j.nucmedbio.2007.12.005 [PubMed: 18355688]
125. Fookes CJ; Pham TQ; Mattner F; Greguric I; Loc'h C; Liu X; Berghofer P; Shepherd R; Gregoire MC; Katsifis A Synthesis and biological evaluation of substituted [^{18}F]imidazo[1,2-a]pyridines and [^{18}F]pyra-zolo[1,5-a]pyrimidines for the study of the peripheral benzodiazepine receptor using positron emission tomography.J. Med. Chem, 2008, 51(13), 3700–3712. 10.1021/jm7014556 [PubMed: 18557607]
126. Perrone M; Moon BS; Park HS; Laquintana V; Jung JH; Cutrignelli A; Lopedota A; Franco M; Kim SE;Lee BC; Denora N A novel PET imaging probe for the detection and monitoring of translocator protein 18 kDa expression in pathological disorders. Sci. Rep, 2016, 6, 20422–20434. 10.1038/srep20422 [PubMed: 26853260]
127. Callaghan PD; Wimberley CA; Rahardjo GL; Berghofer PJ; Pham TQ; Jackson T; Zahra D; Bourdier T; Wyatt N; Greguric I; Howell NR; Siegele R; Pastuovic Z; Mattner F; Loc'h C; Gregoire MC; Katsifis A Comparison of *in vivo* binding properties of the 18-kDa

translocator protein (TSPO) ligands [^{11}F]PBR102 and [^{18}F]PBR111 in a model of excitotoxin-induced neuroinflammation. Eur. J. Nucl. Med. Mol. Imaging, 2015, 42(1), 138–151. 10.1007/s00259-014-2895-3 [PubMed: 25231248]

128. Colasanti A; Guo Q; Muhlert N; Giannetti P; Onega M; Newbould RD; Ciccarelli O; Rison S; Thomas C; Nicholas R; Muraro PA; Malik O; Owen DR; Piccini P; unn RN; Rabiner EA; Matthews PM *In vivo* assessment of brain white matter inflammation in multiple sclerosis with ^{18}F-PBR111 PET. J. Nuclear Med, 2014, 55(7), 1112–1118.

129. Guo Q; Colasanti A; Owen DR; Onega M; Kamalakaran A; Bennacef I; Matthews PM; Rabiner EA; Turkheimer FE; Gunn RN Quantification of the specific translocator protein signal of ^{18}F-PBR111 in healthy humans: A genetic polymorphism effect on *in vivo* binding. J. Nuclear Med, 2013, 54(11), 1915–1923.

130. Kim K; Kim H; Bae SH; Lee SY; Kim YH; Na J;Lee CH; Lee MS; Ko GB; Kim KY; Lee SH; Song IH; Cheon GJ; Kang KW; Kim SE; Chung JK; Kim EE; Paek SH; Lee JS; Lee BC; Youn H [^{18}F]CB251 PET/MR imaging probe targeting translocator protein (TSPO) independent of its polymorphism in a neuroinflammation model. Theranostics, 2020, 10(20), 9315–9331. 10.7150/thno.46875 [PubMed: 32802194]

131. James ML; Fulton RR; Henderson DJ; Eberl S; Meikle SR; Thomson S; Allan RD; Dolle F; Fulham MJ; Kassiou M Synthesis and *in vivo* evaluation of a novel peripheral benzodiazepine receptor PET radioligand. Bioorg. Med. Chem, 2005, 13(22), 6188–6194. 10.1016/j.bmc.2005.06.030 [PubMed: 16039131]

132. James ML; Fulton RR; Vercoullie J; Henderson DJ; Garreau L; Chalon S; Dolle F; Costa B; Guilloteau D; Kassiou M DPA-714, a new translocator protein-specific ligand: synthesis, radiofluorination, and pharmacologic characterization. J. Nuclear Med, 2008, 49(5), 814–822.

133. Chaney A; Cropper HC; Johnson EM; Lechtenberg KJ; Peterson TC; Stevens MY; Buckwalter MS; James ML ^{11}C-DPA-713 *versus*^{18}F-GE-180: A preclinical comparison of translocator protein 18 kDa PET tracers to visualize acute and chronic neuroinflammation in a mouse model of ischemic stroke. J. Nuclear Med, 2019, 60(1), 122–128.

134. Kobayashi M; Jiang T; Telu S; Zoghbi SS; Gunn RN; Rabiner EA; Owen DR; Guo Q; Pike VW; Innis RB; Fujita M ^{11}C-DPA-713 has much greater specific binding to translocator protein 18 kDa (TSPO) in human brain than ^{11}C-(R)-PK11195. J. Cereb. Blood Flow Metab, 2018, 38(3), 393–403. 10.1177/0271678X17699223 [PubMed: 28322082]

135. Chauveau F; Van Camp N; Dollé F; Kuhnast B; Hinnen F; Damont A; Boutin H; James M; Kassiou M; Tavitian B Comparative evaluation of the translocator protein radioligands 11C-DPA-713, ^{18}F-DPA-714, and 11C-PK11195 in a rat model of acute neuroinflammation. J. Nuclear Med, 2009, 50(3), 468–476.

136. Zinnhardt B; Müther M; Roll W; Backhaus P; Jeibmann A; Foray C; Barca C; Döring C; Tavitian B; Dolle F; Weckesser M; Winkeler A; Hermann S; Wagner S; Wiendl H; Stummer W; Jacobs AH; Schäfers M; Grauer OM TSPO imaging-guided characterization of the immunosuppressive myeloid tumor microenvironment in patients with malignant glioma. Neuro-oncol., 2020, 22(7), 1030–1043. 10.1093/neuonc/noaa023 [PubMed: 32047908]

137. Foray C; Valtorta S; Barca C; Winkeler A; Roll W; Müther M; Wagner S; Gardner ML; Hermann S; Schäfers M; Grauer OM; Moresco RM; Zinnhardt B; Jacobs AH Imaging temozolomide-induced changes in the myeloid glioma microenvironment. Theranostics,11(5), 2020–2033. 10.7150/thno.47269

138. Golla SS; Boellaard R; Oikonen V; Hoffmann A; van Berckel BN; Windhorst AD; Virta J; Haaparanta--Solin M; Luoto P; Savisto N; Solin O; Valencia R; Thiele A; Eriksson J; Schuit RC; Lammertsma AA; Rinne JO Quantification of [^{18}F]DPA-714 binding in the human brain: initial studies in healthy controls and Alzheimer's disease patients. J. Cereb. Blood Flow Metab, 2015, 35(5), 766–772. 10.1038/jcbfm.2014.261 [PubMed: 25649991]

139. Hagens MHJ; Golla SV; Wijburg MT; Yaqub M; Heijtel D; Steenwijk MD; Schober P; Brevé JJP; Schuit RC; Reekie TA; Kassiou M; van Dam AM; Windhorst AD; Killestein J; Barkhof F; van Berckel BNM; Lammertsma AA *In vivo* assessment of neuroinflammation in progressive multiple sclerosis: a proof of concept study with [^{18}F]DPA714 PET. J. Neuroinflammation, 2018, 15(1), 314–323. 10.1186/s12974-018-1352-9 [PubMed: 30424780]

140. Niu N; Xing H; Wang X; Ding J; Hao Z; Ren C; Ba J; Zheng L; Fu C; Zhao H; Huo L Comparative [^{18}F]FDG and [^{18}F]DPA714 PET imaging and time-dependent changes of brown adipose tissue in tumour-bearing mice. Adipocyte, 2020, 9(1), 542–549. 10.1080/21623945.2020.1814546 [PubMed: 32902340]

141. Lavisse S; García-Lorenzo D; Peyronneau MA; Bodini B; Thiriez C; Kuhnast B; Comtat C; Remy P; Stankoff B; Bottlaender M Optimized quantification of translocator protein radioligand ^{11}F-DPA-714 uptake in the brain of genotyped healthy volunteers. J. Nuclear Med, 2015, 56(7), 1048–1054.

142. Peyronneau MA; Saba W; Goutal S; Damont A; Dollé F; Kassiou M; Bottlaender M; Valette H Metabolism and quantification of [^{11}F]DPA-714, a new TSPO positron emission tomography radioligand. Drug Metab. Dispos, 2013, 41(1), 122–131. 10.1124/dmd.112.046342 [PubMed: 23065531]

143. Wang L; Cheng R; Fujinaga M; Yang J; Zhang Y; Hatori A; Kumata K; Yang J; Vasdev N; Du Y; Ran C; Zhang MR; Liang SH A facile radiolabeling of [^{18}F]FDPA *via* spirocyclic iodonium ylides: Preliminary PET imaging studies in preclinical models of neuroinflammation. J. Med. Chem, 2017, 60(12), 5222–5227. 10.1021/acs.jmedchem.7b00432 [PubMed: 28530834]

144. Keller T; Krzyczmonik A; Forsback S; Picón FRL; Kirjavainen AK; Takkinen J; Rajander J; Cacheux F; Damont A; Dolle F; Rinne JO; Haaparanta-Solin M; Solin O Radiosynthesis and preclinical evaluation of [^{18}F]F-DPA, a novel pyrazolo[1,5a]pyrimidine Acetamide TSPO radioligand, in healthy sprague dawley rats. Mol. Imaging Biol, 2017, 19(5), 736–745. 10.1007/s11307-016-1040-z [PubMed: 28083825]

145. Keller T; López-Picón FR; Krzyczmonik A; Forsback S; Kirjavainen AK; Takkinen JS; Alzghool O; Rajander J; Teperi S; Cacheux F; Damont A; Dollé F; Rinne JO; Solin O; Haaparanta-Solin M [^{18}F]F-DPA for the detection of activated microglia in a mouse model of Alzheimer's disease. Nucl. Med. Biol, 2018, 67, 1–9. 10.1016/j.nucmedbio.2018.09.001 [PubMed: 30317069]

146. Keller T; López-Picón FR; Krzyczmonik A; Forsback S; Takkinen JS; Rajander J; Teperi S; Dollé F; Rinne JO; Haaparanta-Solin M; Solin O Comparison of high and low molar activity TSPO tracer [^{18}F]F-DPA in a mouse model of Alzheimer's disease. J. Cereb. Blood Flow Metab, 2020, 40(5), 1012–1020. 10.1177/0271678X19853117 [PubMed: 31142224]

147. Tang D; McKinley ET; Hight MR; Uddin MI; Harp JM; Fu A; Nickels ML; Buck JR; Manning HC Synthesis and structure-activity relationships of 5,6,7-substituted pyrazolopyrimidines: discovery of a novel TSPO PET ligand for cancer imaging. J. Med. Chem, 2013, 56(8), 3429–3433. 10.1021/jm4001874 [PubMed: 23521048]

148. Tang D; Nickels ML; Tantawy MN; Buck JR; Manning HC Preclinical imaging evaluation of novel TSPO-PET ligand 2-(5,7-Diethyl-2-(4-(2-[^{11}F]fluoroethoxy) phenyl)pyrazolo[1,5-a]pyrimidin-3-yl)-N,N-diethylacetamide ([^{18}F]VUIIS1008) in glioma. Mol. Imaging Biol, 2014, 16(6), 813–820. 10.1007/s11307-014-0743-2 [PubMed: 24845529]

149. Pulagam KR; Colás L; Padro D; Plaza-García S; Gómez-Vallejo V; Higuchi M; Llop J; Martín A Evaluation of the novel TSPO radiotracer [^{18}F] VUIIS1008 in a preclinical model of cerebral ischemia in rats. EJNMMI Res., 2017, 7(1), 93–105. 10.1186/s13550-017-0343-7 [PubMed: 29177913]

150. Tang D; Fujinaga M; Hatori A; Zhang Y; Yamasaki T; Xie L; Mori W; Kumata K; Liu J; Manning HC; Huang G; Zhang MR Evaluation of the novel TSPO radiotracer 2-(7-butyl-2-(4-(2-([^{18}F]fluoroethoxy)phenyl)-5-methylpyrazolo[1,5-a]pyrimidin-3-yl)-N,N-diethylacetamide in a preclinical model of neuroinflammation. Eur. J. Med. Chem, 2018, 150, 1–8. 10.1016/j.ejmech.2018.02.076 [PubMed: 29505933]

151. Tang D; Li J; Nickels ML; Huang G; Cohen AS; Manning HC Preclinical evaluation of a novel TSPO PET Ligand 2-(7-Butyl-2-(4-(2-[^{18}F]Fluoroethoxy) phenyl)-5-methylpyrazolo[1,5-a]pyrimidin-3-yl)-N,N-di-ethylacetamide (^{18}F-VUIIS1018A) to image glioma. Mol. Imaging Biol, 2019, 21(1), 113–121. 10.1007/s11307-018-1198-7 [PubMed: 29869061]

152. Kozikowski AP; Ma D; Brewer J; Sun S; Costa E; Romeo E; Guidotti A Chemistry, binding affinities, and behavioral properties of a new class of "antineophobic" mitochondrial DBI receptor complex (mDRC) ligands. J. Med. Chem, 1993, 36(20), 2908–2920. 10.1021/jm00072a010 [PubMed: 8411007]

153. Primofiore G; Da Settimo F; Taliani S; Simorini F; Patrizi MP; Novellino E; Greco G; Abignente E; Costa B; Chelli B; Martini C N,N-dialkyl-2-phenylindol-3-ylglyoxylamides. A new class of potent and selective ligands at the peripheral benzodiazepine receptor. J. Med. Chem, 2004, 47(7), 1852–1855. 10.1021/jm030973k [PubMed: 15027878]

154. Da Settimo F; Simorini F; Taliani S; La Motta C; Marini AM; Salerno S; Bellandi M; Novellino E; Greco G; Cosimelli B; Da Pozzo E; Costa B; Simola N; Morelli M; Martini C Anxiolytic-like effects of N,N--dialkyl-2-phenylindol-3-ylglyoxylamides by modulation of translocator protein promoting neurosteroid biosynthesis. J. Med. Chem, 2008, 51(18), 5798–5806. 10.1021/jm8003224 [PubMed: 18729350]

155. Pike VW; Taliani S; Lohith TG; Owen DR; Pugliesi I; Da Pozzo E; Hong J; Zoghbi SS; Gunn RN; Parker CA; Rabiner EA; Fujita M; Innis RB; Martini C; Da Settimo F Evaluation of novel N1-methyl-2-phenylindol-3-ylglyoxylamides as a new chemotype of 18 kDa translocator protein-selective ligand suitable for the development of positron emission tomography radioligands. J. Med. Chem, 2011, 54(1), 366–373. 10.1021/jm101230g [PubMed: 21133364]

156. Ferzaz B; Brault E; Bourliaud G; Robert JP; Poughon G; Claustre Y; Marguet F; Liere P; Schumacher M; Nowicki JP; Fournier J; Marabout B; Sevrin M; George P; Soubrie P; Benavides J; Scatton B SSR180575 (7-chloro-N,N,5-trimethyl-4-oxo-3-phenyl-3,5-dihydro-4H-pyridazino[4,5-b]indole-1-acetamide), a peripheral benzodiazepine receptor ligand, promotes neuronal survival and repair. J. Pharmacol. Exp. Ther, 2002, 301(3), 1067–1078. 10.1124/jpet.301.3.1067 [PubMed: 12023539]

157. Thominiaux C; Damont A; Kuhnast B; Demphel S; Le Helleix S; Boisnard S; Rivron L; Chauveau F; Boutin H; Van Camp N; Boisgard R; Roy S; Allen J; Rooney T; Benavides J; Hantraye P; Tavitian B; Dollé F Radiosynthesis of 7-chloro-N,N-dimethyl-5-[^{11}C] methyl-4-oxo-3-phenyl-3,5-dihydro-4H-pyridazino[4, 5-b]indole-1-acetamide, [^{11}C]SSR180575, a novel radioligand for imaging the TSPO (peripheral benzodiazepine receptor) with PET. J. Labelled Comp. Radiopharm, 2010, 53(13), 767–773. 10.1002/jlcr.1794

158. Chauveau F; Boutin H; Van Camp N; Thominiaux C; Hantraye P; Rivron L; Marguet F; Castel MN; Rooney T; Benavides J; Dollé F; Tavitian B *In vivo* imaging of neuroinflammation in the rodent brain with [^{11}C]SSR180575, a novel indoleacetamide radioligand of the translocator protein (18 kDa). Eur. J. Nucl. Med. Mol. Imaging, 2011, 38(3), 509–514. 10.1007/s00259-010-1628-5 [PubMed: 20936410]

159. Cheung YY; Nickels ML; Tang D; Buck JR; Manning HC Facile synthesis of SSR180575 and discovery of 7-chloro-N,N,5-trimethyl-4-oxo-3(6-[^{11}F]fluoropyridin-2-yl)-3,5-dihydro-4H-pyridazino[4,5-b]indole-1-acetamide, a potent pyridazinoindole ligand for PET imaging of TSPO in cancer. Bioorg. Med. Chem. Lett, 2014, 24(18), 4466–4471. 10.1016/j.bmcl.2014.07.091 [PubMed: 25172419]

160. Okubo T; Yoshikawa R; Chaki S; Okuyama S; Nakazato A Design, synthesis, and structure-activity relationships of novel tetracyclic compounds as peripheral benzodiazepine receptor ligands. Bioorg. Med. Chem, 2004, 12(13), 3569–3580. 10.1016/j.bmc.2004.04.025 [PubMed: 15186841]

161. Wadsworth H; Jones PA; Chau WF; Durrant C; Fouladi N; Passmore J; O'Shea D; Wynn D; Morisson-Iveson V; Ewan A; Thaning M; Mantzilas D; Gausemel I; Khan I; Black A; Avory M; Trigg W [^{1} F]GE-180: a novel fluorine-18 labelled PET tracer for imaging Translocator protein 18 kDa (TSPO). Bioorg. Med. Chem. Lett, 2012, 22(3), 1308–1313. 10.1016/j.bmcl.2011.12.084 [PubMed: 22244939]

162. Chau WF; Black AM; Clarke A; Durrant C; Gausemel I; Khan I; Mantzilas D; Oulie I; Rogstad A; Trigg W; Jones PA Exploration of the impact of stereochemistry on the identification of the novel translocator protein PET imaging agent [^{11}F]GE-180. Nucl. Med. Biol, 2015, 42(9), 711–719. 10.1016/j.nucmedbio.2015.05.004 [PubMed: 26072270]

163. Dickens AM; Vainio S; Marjamäki P; Johansson J; Lehtiniemi P; Rokka J; Rinne J; Solin O; Haaparanta--Solin M; Jones PA; Trigg W; Anthony DC; Airas L Detection of microglial activation in an acute model of neuroinflammation using PET and radiotracers 11C-(R)-PK11195 and ^{18}F-GE-180. J. Nuclear Med, 2014, 55(3), 466–472.

164. Boutin H; Murray K; Pradillo J; Maroy R; Smigova A; Gerhard A; Jones PA; Trigg W ^{18}F-GE-180: A novel TSPO radiotracer compared to 11C-R-PK11195 in a preclinical model of

stroke. Eur. J. Nucl. Med. Mol. Imaging, 2015, 42(3), 503–511. 10.1007/s00259-014-2939-8 [PubMed: 25351507]

165. Liu B; Le KX; Park MA; Wang S; Belanger AP; Dubey S; Frost JL; Holton P; Reiser V; Jones PA; Trigg W; Di Carli MF; Lemere CA *In vivo* detection of age- and disease-related increases in neuroinflammation by ^{18}F-GE180 TSPO MicroPET imaging in wild-type and Alzheimer's transgenic mice. J. Neurosci, 2015, 35(47), 15716–15730. 10.1523/JNEUROSCI.0996-15.2015 [PubMed: 26609163]
166. Feeney C; Scott G; Raffel J; Roberts S; Coello C; Jolly A; Searle G; Goldstone AP; Brooks DJ; Nicholas RS; Trigg W; Gunn RN; Sharp DJ Kinetic analysis of the translocator protein positron emission tomography ligand [^{18}F]GE-180 in the human brain. Eur. J. Nucl. Med. Mol. Imaging, 2016, 43(12), 2201–2210. 10.1007/s00259-016-3444-z [PubMed: 27349244]
167. Fan Z; Calsolaro V; Atkinson RA; Femminella GD; Waldman A; Buckley C; Trigg W; Brooks DJ; Hinz R; Edison P Flutriciclamide (^{18}F-GE180) PET: First-in Human PET study of novel third-generation *in vivo* marker of human translocator protein. J. Nuclear Med, 2016, 57(11), 1753–1759.
168. Unterrainer M; Mahler C; Vomacka L; Lindner S; Havla J; Brendel M; Böning G; Ertl-Wagner B; Kumpfel T; Milenkovic VM; Rupprecht R; Kerschen-steiner M; Bartenstein P; Albert NL TSPO PET with [^{18}F]GE-180 sensitively detects focal neuroinflammation in patients with relapsing-remitting multiple sclerosis. Eur. J. Nucl. Med. Mol. Imaging, 2018, 45(8), 1423–1431. 10.1007/s00259-018-3974-7 [PubMed: 29523925]
169. Albert NL; Unterrainer M; Fleischmann DF; Lindner S; Vettermann F; Brunegraf A; Vomacka L; Brendel M; Wenter V; Wetzel C; Rupprecht R; Tonn JC; Belka C; Bartenstein P; Niyazi M TSPO PET for glioma imaging using the novel ligand ^{18}F-GE-180: first results in patients with glioblastoma. Eur. J. Nucl. Med. Mol. Imaging, 2017, 44(13), 2230–2238. 10.1007/s00259-017-3799-9 [PubMed: 28821920]
170. Unterrainer M; Fleischmann DF; Diekmann C; Vomacka L; Lindner S; Vettermann F; Brendel M; Wenter V; Ertl-Wagner B; Herms J; Wetzel C; Rupprecht R; Tonn JC; Belka C; Bartenstein P; Niyazi M; Albert NL Comparison of ^{18}F-GE-180 and dynamic ^{18}F-FET-PET in high grade glioma: A double-tracer pilot study. Eur. J. Nucl. Med. Mol. Imaging, 2019, 46(3), 580–590. 10.1007/s00259-018-4166-1 [PubMed: 30244386]
171. Unterrainer M; Fleischmann DF; Lindner S; Brendel M; Rupprecht R; Tonn JC; Belka C; Bartenstein P; Niyazi M; Albert NL Detection of cerebrospinal fluid dissemination of recurrent glioblastoma using TSPO-PET With ^{18}F-GE-180. Clin. Nucl. Med, 2018, 43(7), 518–519. 10.1097/RLU.0000000000002113 [PubMed: 29742608]
172. Unterrainer M; Fleischmann DF; Vettermann F; Ruf V; Kaiser L; Nelwan D; Lindner S; Brendel M; Wenter V; Stöcklein S; Herms J; Milenkovic VM; Rupprecht R; Tonn JC; Belka C; Bartenstein P; Niyazi M; Albert NL TSPO PET, tumour grading and molecular genetics in histologically verified glioma: a correlative ^{18}F-GE-180 PET study. Eur. J. Nucl. Med. Mol. Imaging, 2020, 47(6), 1368–1380. 10.1007/s00259-019-04491-5 [PubMed: 31486876]
173. Roncaroli F; Su Z; Herholz K; Gerhard A; Turkheimer FE TSPO expression in brain tumours: Is TSPO a target for brain tumour imaging? Clin. Transl. Imaging, 2016, 4, 145–156. 10.1007/s40336-016-0168-9 [PubMed: 27077069]
174. Zanotti-Fregonara P; Pascual B; Rizzo G; Yu M; Pal N; Beers D; Carter R; Appel SH; Atassi N; Masdeu JC Head-to-Head Comparison of ^{11}C-PBR28 and ^{18}F-GE180 for quantification of the translocator protein in the human brain. J. Nuclear Med, 2018, 59(8), 1260–1266.
175. Zanotti-Fregonara P; Pascual B; Rostomily RC; Rizzo G; Veronese M; Masdeu JC; Turkheimer F Anatomy of ^{18}F-GE180, a failed radioligand for the TSPO protein. Eur. J. Nucl. Med. Mol. Imaging, 2020, 47(10), 2233–2236. 10.1007/s00259-020-04732-y [PubMed: 32088848]
176. Qiao L; Fisher E; McMurray L; Milicevic Sephton S; Hird M; Kuzhuppilly-Ramakrishnan N; Williamson DJ; Zhou X; Werry E; Kassiou M; Luthra S; Trigg W ; Aigbirhio FI Radiosynthesis of (R,S)-[^{18} F]GE387: A Potential PET Radiotracer for Imaging Translocator Protein 18 kDa (TSPO) with low binding sensitivity to the human gene polymorphism rs6971. ChemMedChem, 2019, 14(9), 982–993. 10.1002/cmdc.201900023 [PubMed: 30900397]

177. Zhang MR; Kumata K; Maeda J; Yanamoto K; Hatori A; Okada M; Higuchi M; Obayashi S; Suhara T; Suzuki K 11C-AC-5216: A novel PET ligand for peripheral benzodiazepine receptors in the primate brain. J. Nuclear Med, 2007, 48(11), 1853–1861.

178. Maeda J; Zhang MR; Okauchi T; Ji B; Ono M; Hattori S; Kumata K; Iwata N; Saido TC; Trojanowski JQ; Lee VM; Staufenbiel M; Tomiyama T; Mori H; Fukumura T; Suhara T; Higuchi M *In vivo* positron emission tomographic imaging of glial responses to amyloid-beta and tau pathologies in mouse models of Alzheimer's disease and related disorders. J. Neurosci, 2011, 31(12), 4720–4730. 10.1523/JNEUROSCI.3076-10.2011 [PubMed: 21430171]

179. Rupprecht R; Papadopoulos V; Rammes G; Baghai TC; Fan J; Akula N; Groyer G; Adams D; Schumacher M Translocator protein (18 kDa) (TSPO) as a therapeutic target for neurological and psychiatric disorders. Nat. Rev. Drug Discov, 2010, 9(12), 971–988. 10.1038/nrd3295 [PubMed: 21119734]

180. Gong J; Szego ÉM; Leonov A; Benito E; Becker S; Fischer A; Zweckstetter M; Outeiro T; Schneider A Translocator protein ligand protects against neurodegeneration in the MPTP mouse model of parkinsonism. J. Neurosci, 2019, 39(19), 3752–3769 10.1523/JNEUROSCI.2070-18.2019 [PubMed: 30796158]

181. Owen DR; Lewis AJ; Reynolds R; Rupprecht R; Eser D; Wilkins MR; Bennacef I; Nutt DJ; Parker CA Variation in binding affinity of the novel anxiolytic XBD173 for the 18 kDa translocator protein in human brain. Synapse, 2011, 65(3), 257–259. 10.1002/syn.20884 [PubMed: 21132812]

182. Yanamoto K; Yamasaki T; Kumata K; Yui J; Odawara C; Kawamura K; Hatori A; Inoue O; Yamaguchi M; Suzuki K; Zhang MR Evaluation of N-benzyl-N-[^{11}C]methyl-2- (7-methyl-8-oxo-2-phenyl-7,8-dihydro-9H-purin-9-yl)acetamide ([^{11}C]DAC) as a novel translocator protein (18 kDa) radioligand in kainic acid-lesioned rat. Synapse, 2009, 63(11), 961–971. 10.1002/syn.20678 [PubMed: 19593823]

183. Yui J; Hatori A; Kawamura K; Yanamoto K; Yamasaki T; Ogawa M; Yoshida Y; Kumata K; Fujinaga M; Nengaki N; Fukumura T; Suzuki K; Zhang MR Visualization of early infarction in rat brain after ischemia using a translocator protein (18 kDa) PET ligand [^{11}C]DAC with ultra-high specific activity. Neuroimage, 2011, 54(1), 123–130. 10.1016/j.neuroimage.2010.08.010 [PubMed: 20705143]

184. Yanamoto K; Kumata K; Yamasaki T; Odawara C; Kawamura K; Yui J; Hatori A; Suzuki K; Zhang MR [^{18}F]FEAC and [^{18}F]FEDAC: Two novel positron emission tomography ligands for peripheral-type benzodiazepine receptor in the brain. Bioorg. Med. Chem. Lett, 2009, 19(6), 1707–1710. 10.1016/j.bmcl.2009.01.093 [PubMed: 19217778]

185. Yui J; Maeda J; Kumata K; Kawamura K; Yanamoto K; Hatori A; Yamasaki T; Nengaki N; Higuchi M; Zhang MR ^{18}F-FEAC and ^{18}F-FEDAC: PET of the monkey brain and imaging of translocator protein (18 kDa) in the infarcted rat brain. J. Nuclear Med, 2010, 51(8), 1301–1309.

186. Chung SJ; Yoon HJ; Youn H; Kim MJ; Lee YS; Jeong JM; Chung JK; Kang KW; Xie L; Zhang MR; Cheon GJ ^{18}F-FEDAC as a targeting agent for activated macrophages in DBA/1 mice with collagen-induced arthritis: Comparison with ^{18}F-FDG. J. Nuclear Med, 2018, 59(5), 839–845.

187. Tiwari AK; Yui J; Fujinaga M; Kumata K; Shimoda Y; Yamasaki T; Xie L; Hatori A; Maeda J; Nengaki N; Zhang MR Characterization of a novel acetamidobenzoxazolone-based PET ligand for translocator protein (18 kDa) imaging of neuroinflammation in the brain. J. Neurochem, 2014, 129(4), 712–720. 10.1111/jnc.12670 [PubMed: 24484439]

188. Tiwari AK; Fujinaga M; Yui J; Yamasaki T; Xie L; Kumata K; Mishra AK; Shimoda Y; Hatori A; Ji B; Ogawa M; Kawamura K; Wang F; Zhang MR Synthesis and evaluation of new ^{18}F-labelled acetamidobenzoxazolone-based radioligands for imaging of the translocator protein (18 kDa, TSPO) in the brain. Org. Biomol. Chem, 2014, 12(47), 9621–9630. 10.1039/C4OB01933D [PubMed: 25339090]

189. Tiwari AK; Ji B; Yui J; Fujinaga M; Yamasaki T; Xie L; Luo R; Shimoda Y; Kumata K; Zhang Y; Hatori A; Maeda J; Higuchi M; Wang F; Zhang MR [^{18}F]FEBMP: Positron Emission Tomography Imaging ofSPO in a model of neuroinflammation in rats, and *in vitro* autoradiograms of the human brain. Theranostics, 2015, 5(9), 961–969. 10.7150/thno.12027 [PubMed: 26155312]

190. Fujinaga M; Luo R; Kumata K; Zhang Y; Hatori A; Yamasaki T; Xie L; Mori W; Kurihara Y; Ogawa M; Nengaki N; Wang F; Zhang MR Development of a ^{18}F-Labeled radiotracer with improved brain kinetics for positron emission tomography imaging of translocator protein (18 kDa) in ischemic brain and glioma. J. Med. Chem, 2017, 60(9), 4047–4061. 10.1021/acs.jmedchem.7b00374 [PubMed: 28422499]

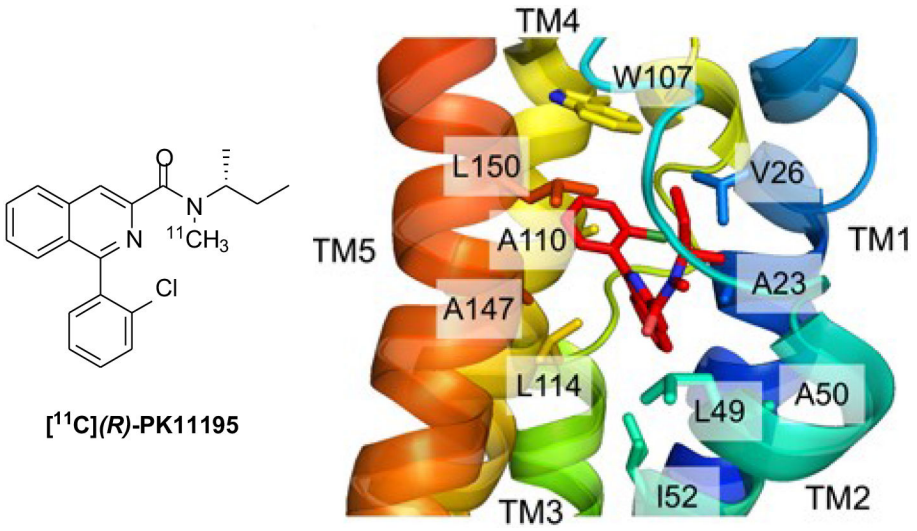

Fig.(1).

Structure of [^{11}C](*R*)-PK11175 (left panel) and detailed view of its positioning in the binding cavity (residues forming the binding cavity are shown in a stick representation, transmembrane helices are color coded) (right panel); reproduced and adapted from [5] with permission. (*A higher resolution / colour version of this figure is available in the electronic copy of the article*).

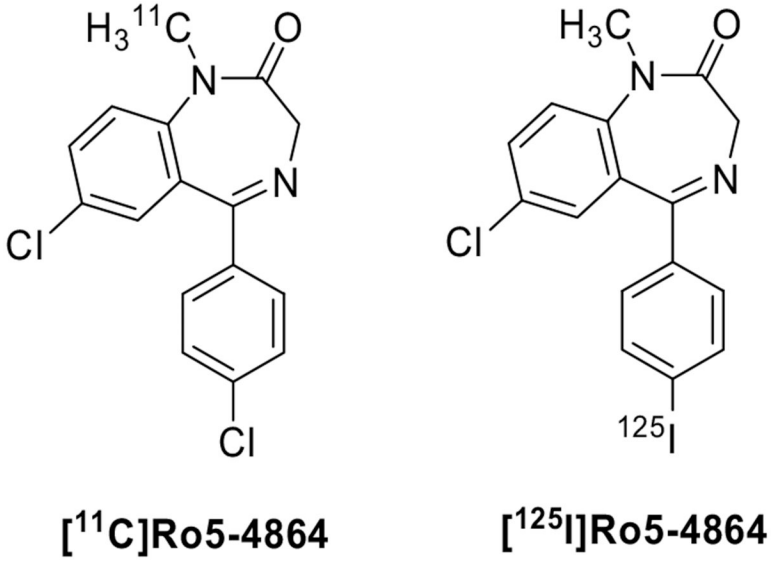

Fig. (2).
Structures of benzodiazepines as TSPO radioligands.

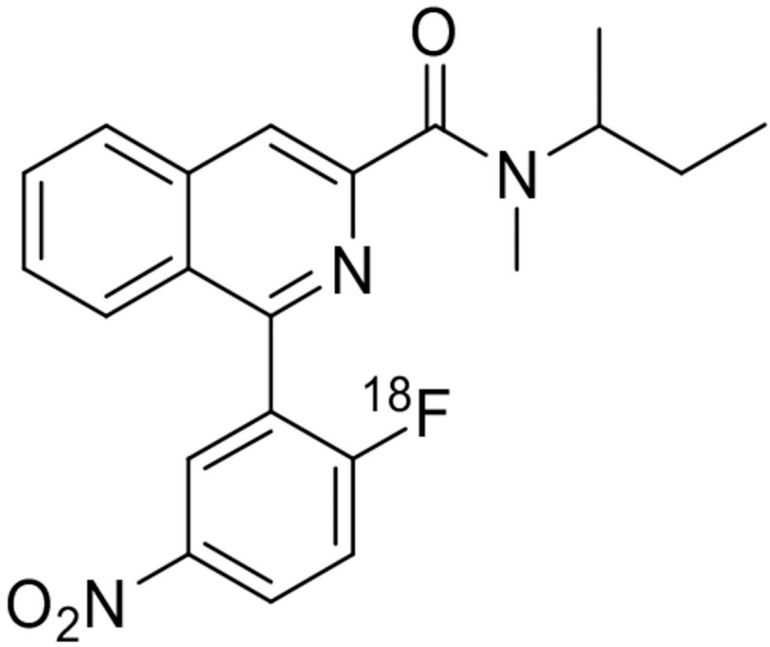

[18F]PK14105

Fig. (3).
Structure of [18F]PK14105.

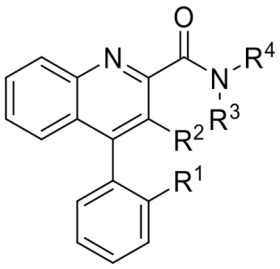

	R^1	R^2	R^3	R^4
[^{11}C]VC193M	H	CH_3	$^{11}CH_3$	$CH(CH_3)CH_2CH_3$
[^{11}C]VC198M	F	CH_3	$^{11}CH_3$	$CH(CH_3)CH_2CH_3$
[^{11}C]VC195	H	CH_3	$^{11}CH_3$	CH_2Ph
[^{11}C]VC701	H	CH_2F	$^{11}CH_3$	CH_2Ph
[^{18}F]VC701	H	$CH_2{}^{18}F$	CH_3	CH_2Ph

Fig. (4).
Structures of quinoline-2-carboxamides as TSPO radioligands.

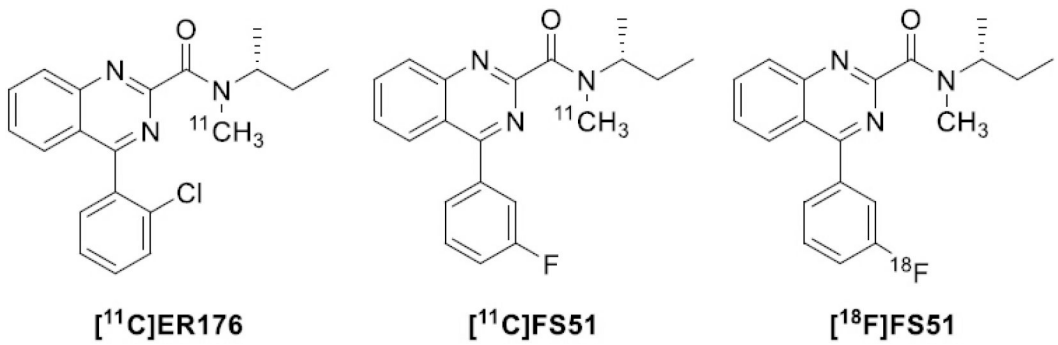

Fig. (5).
Structures of the quinazoline TSPO radioligands [^{11}C]ER176, [^{11}C]FS51, and [^{18}F]FS51.

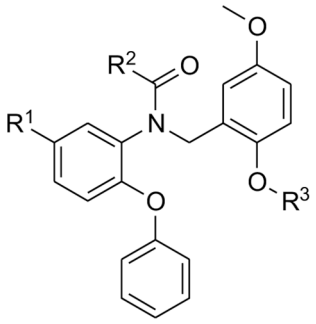

	R^1	R^2	R^3
[^{11}C]DAA1106	F	CH_3	$^{11}CH_3$
[^{18}F]DAA1106	^{18}F	CH_3	CH_3
[^{18}F]FMDAA1106	F	CH_3	$CH_2{}^{18}F$
[^{18}F]FEDAA1106	F	CH_3	$(CH_2)_2{}^{18}F$
[^{18}F]PBR06	H	$CH_2{}^{18}F$	CH_3

Fig. (6).
Structures of the phenoxyphenylacetamides TSPO radioligands.

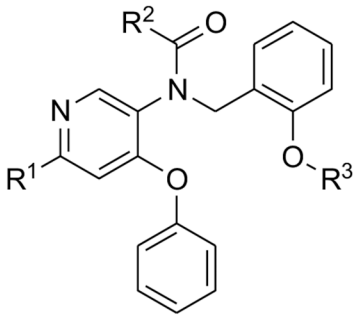

	R^1	R^2	R^3
[^{11}C]PBR28	H	CH_3	$^{11}CH_3$
[^{18}F]FMPBR28	H	CH_3	$CH_2{}^{18}F$
[^{18}F]FEPPA	H	CH_3	$(CH_2)_2{}^{18}F$
[^{18}F]6F-PBR28	^{18}F	CH_3	CH_3

Fig. (7).
Structures of the phenoxypyridinylacetamides TSPO radioligands.

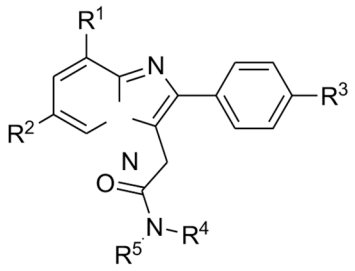

	R^1	R^2	R^3	R^4	R^5
Alpidem	H	Cl	Cl	Pr	Pr
[^{11}C]CLINME	H	Cl	I	Et	$^{11}CH_3$
[^{123}I]CLINME	H	Cl	^{123}I	Et	CH_3
[^{11}C]PBR170	Cl	Cl	OCH_3	2-F-Py	$^{11}CH_3$
[^{11}C]CB148	Cl	Cl	Cl	Ph	$^{11}CH_3$
[^{18}F]PBR111	H	Cl	$O(CH_2)_3{}^{18}F$	Et	Et
[^{18}F]PBR102	H	Cl	$O(CH_2)_2{}^{18}F$	Et	Et
[^{18}F]CB251	Cl	Cl	$O(CH_2)_2{}^{18}F$	Pr	Pr

Fig. (8).
Structures of the imidazo[1,2-*a*]pyridines TSPO radioligands.

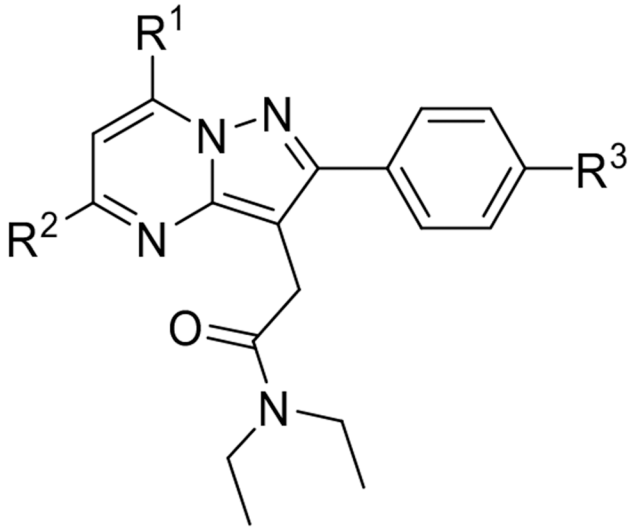

	R^1	R^2	R^3
[^{11}C]DPA713	CH_3	CH_3	$O^{11}CH_3$
[^{18}F]DPA714	CH_3	CH_3	$OCH_2CH_2{}^{18}F$
[^{18}F]FDPA	CH_3	CH_3	^{18}F
[^{18}F]VUIISS1008	Et	Et	$OCH_2CH_2{}^{18}F$
[^{18}F]VUIISS1008A	Bu	CH_3	$OCH_2CH_2{}^{18}F$

Fig. (9).
Structures of the pyrazolo[1,5-*a*]pyrimidine TSPO radioligands.

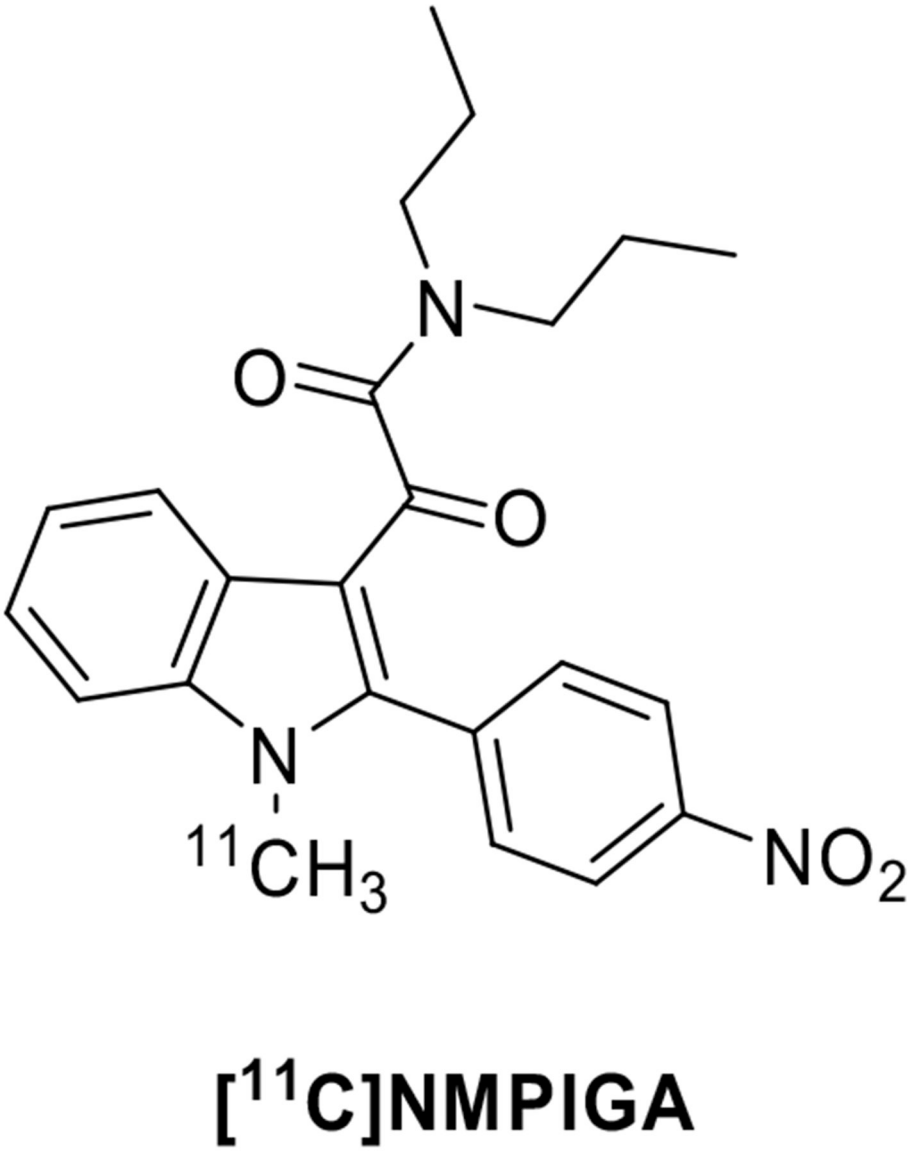

Fig. (10).
Structure of the 2-phenylindole glyoxylamide TSPO radioligand [^{11}C]NMPIGA.

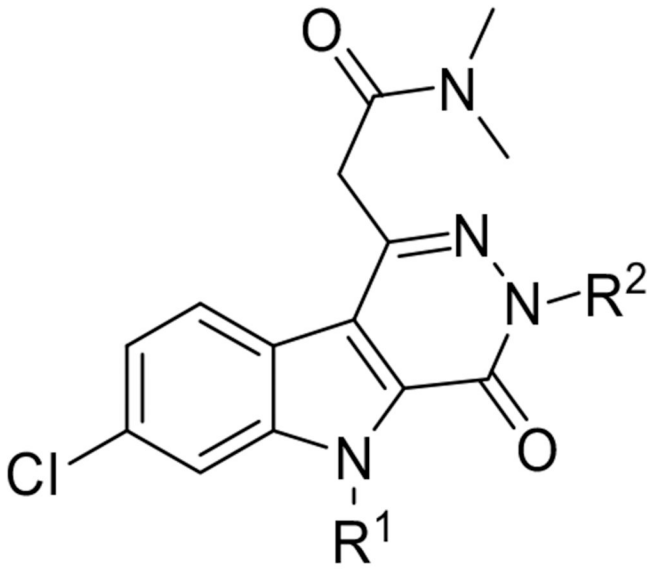

	R^1	R^2
[^{11}C]SSR180575	$^{11}CH_3$	Ph
[^{11}C]FPSSR180575	CH_3	3-^{18}F-Py

Fig. (11).
Structures of the pyridazino[4,5-*b*]indole-5-acetamides TSPO radioligands.

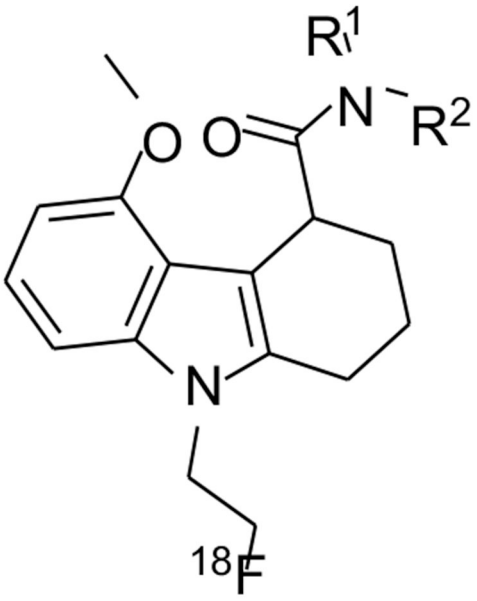

	R^1	R^2
[^{18}F]GE180	CH_2CH_3	CH_2CH_3
[^{18}F]GE387	CH_2CH_3	CH_2Ph

Fig. (12).
Structures of the 2,3,4,9-tetrahydro-carbazole-4--carboxamide TSPO radioligands.

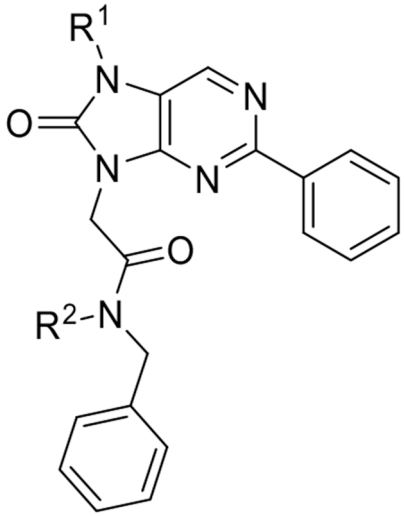

	R^1	R^2
[^{11}C]AC5216	$^{11}CH_3$	Et
[^{11}C]DAC	CH_3	$^{11}CH_3$
[^{18}F]FEAC	$CH_2CH_2{}^{18}F$	Et
[^{18}F]FEDAC	$CH_2CH_2{}^{18}F$	CH_3
[^{18}F]FAC	CH_3	$CH_2CH_2{}^{18}F$

Fig. (13).
Structures of the 8-oxodihydropurines TSPO radioligands.

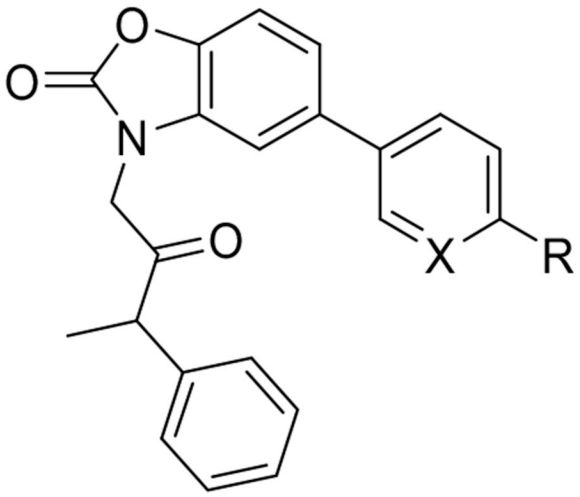

	X	R
[^{11}C]MBMP	CH	$O^{11}CH_3$
[^{18}F]FEBMP	CH	$O(CH_2)_2{}^{18}F$
[^{18}F]FPBMP	CH	$O(CH_2)_3{}^{18}F$
[^{18}F]FPyBMP	N	^{18}F

Fig. (14).
Structures of the benzoxazolones TSPO radioligands.

Table 1.

Chemical classes of TSPO radioligands, their lipophilicity, and binding properties.

Chemical Class	Representative Compounds	Lipophilicity	Affinity [b]	Sensitivity SNP[c]	Refs.
Isoquinolinecarboxamides	[^{11}C]PK11195	log*D* = 3.97	9.1	0.8	[44, 61]
Quinoline-2-carboxamides	[^{11}C]VC195	clog*D* = 4.28 [a]	2.1	n.r.[d]	[72]
	[^{11}C]VC701	clog*D* = 3.97 [a]	0.11	n.r.[d]	[74]
Quinazolines-2-carboxamides	[^{11}C]ER176	log*D* = 3.55	3.1	0.8	[76, 79]
Phenoxyphenylacetamides	[^{11}C]DAA1106	log*P* = 3.65	0.043	4.7	[86, 111]
	[^{18}F]PBR06	log*D* = 4.01	0.18	17	[97, 111]
Phenoxypyridinylacetamides	[^{11}C]PBR28	clog*D* = 2.95	0.68	55	[102, 111]
	[^{18}F]FEPPA	log*D* = 2.99	0.07	n.r.[d,e]	[114, 116]
Imidazo[1,2-*a*]pyridines	[^{18}F]PBR111	log*P* = 3.2	3.7	4.0	[125, 111]
	[^{18}F]CB251	log*D* = 3.00	0.27	1.14	[126, 130]
Pyrazolo[1,5-*a*]pyrimidine	[^{11}C]DPA713	log*D* = 2.44	4.7	4.4	[131, 111]
	[^{18}F]DPA714	log*D* = 2.44	7.0	n.r.[d, e]	[132, 141]
Indoles	[^{11}C]NMPIGA	clog*P* = 3.95	5.7	6.0	[153, 155]
	[^{18}F]GE180	logD = 2.95	0.87	15.0	[161, 166]
8-Oxodihydropurines	[^{11}C]AC5216	logD = 3.3	0.2	12.5	[177, 181]
Benzoxazolones	[^{18}F]FEBMP	log*D* = 3.4	6.6	0.9	[188, 189]

[a] clog*D* value calculated by authors with Calculated with ADMETlab 2.0 (https://admetmesh.scbdd.com/).

[b] Affinities (K_i values, nM) of ligands for TSPO in rat brain homogenates

[c] K_i ratios of the ligand for LAB to that of HAB

[d] n.r. = different binding ratios not reported

[e] sensitivity to rs6971 SNP established *in vivo* as described in the reference